Electronic Supplementary Material (ESI) for Chemical Science.
This journal is © The Royal Society of Chemistry 2022

Electronic Supplementary Information for:

Long-lived Charge-Separated State of Spiro Compact Electron Donor-Acceptor Dyads Based on Rhodamine and Naphthalenediimide Chromophores

Xiao Xiao,[a,§] Ivan Kurganskii,[b,§] Partha Maity,[c,§]Jianzhang Zhao,*[,a,d] Xiao Jiang,[e,*] Omar F. Mohammed*[,c] and Matvey Fedin*[,b]

[a] State Key Laboratory of Fine Chemicals, Frontiers Science Center for Smart Materials, School of Chemical Engineering, Dalian University of Technology, Dalian 116024, P. R. China. *E-mail: zhaojzh@dlut.edu.cn

[b] International Tomography Center, SB RAS Institutskaya Str., 3A, and Novosibirsk State University, Pirogova str. 2, Novosibirsk 630090, Russia. *E-mail: mfedin@tomo.nsc.ru

[c] Division of Physical Sciences and Engineering, King Abdullah University of Science and Technology (KAUST), Thuwal 23955-6900, Kingdom of Saudi Arabia. *E-mail: omar.abdelsaboor@kaust.edu.sa

[d] State Key Laboratory of Chemistry and Utilization of Carbon Based Energy Resources, College of Chemistry, Xinjiang University, Urumqi 830017, P. R. China

[e] Key Laboratory of Industrial Ecology and Environmental Engineering (Ministry of Education), School of Environmental Science and Technology, Dalian University of Technology, Dalian 116024, P. R. China. *E-mail: xjiang@dlut.edu.cn

[§] These authors contributed equally to this work.

Contents

1. General Information and Synthesis S3
2. Molecular Structure Characterization Data S4
3. Crystallographic Data S14
4. Steady State UV–vis Absorption Spectra S15
5. Fluorescence Spectra and Fluorescence Lifetimes S16
6. Electrochemical Studies S17
7. Chemical Redox and Spectroelectrochemistry Study S18
8. Femtosecond Transient Absorption Spectroscopy S22
9. Nanosecond Transient Absorption Spectroscopy S24
10. Charge Transfer Quantum Yield S38
11. Time-Resolved Electron Paramagnetic Resonance Spectroscopy S40
12. DFT Calculations S43
13. Photophysical Process S47
14. Coordinates of the optimized Geometries of the Compounds S49
15. References S58

1. General Information and Synthesis

All the chemicals used in synthesis are analytically pure and were used as received, the solvents were dried and distilled before synthesis. ^{1}H and ^{13}C NMR spectra were recorded on the Bruker Avance spectrometers (400 MHz, 500 MHz or 600 MHz). The mass spectra were measured by EI-TOF-HRMS spectrometer. Fourier transform infrared (FT-IR) spectra were recorded using a ThermoFisher Nicolet Nexus 6700 FT-IR spectrometer.

Compounds **NDI**, **4**, **dBr-NDI** and **Rho-Ph** were synthesized following the reported method.[1,2]

Synthesis of 1. Under N_2 atmosphere, 1,4,5,8-naphthalenetetracarboxylic acid dianhydride (2.14 g, 8.0 mmol) was taken in water (350 mL) followed by the addition of 1 M aqueous KOH solution (40 mL). This mixture was vigorously stirred and heated until almost the compound was dissolved. The pH of the resultant solution was acidified to 6~7 by adding 1 M H_3PO_4. To this solution, *n*-butyl amine (1.14 ml, 8.8 mmol) was added and the pH of the solution was readjusted to 6~7 with 1 M H_3PO_4. The mixture was heated to reflux overnight. The mixture was cooled to room temperature and filtered. Then acetic acid (10 mL) was added to the filtrate, the solid precipitate was formed and then filtrated. The solid was dried under vacuum to afford the pale yellow powder (1.12 g, yield: 40%). The product was directly used for the next step without further purification.

Synthesis of 2. Under N_2 atmosphere, 1,4-phenylenediamine (134.0 mg, 1.24 mmol) was dissolved in DMF (10 mL). Then the solution of compound **1** (454.8 mg, 1.2 mmol) in DMF (10 mL) was added dropwise and the mixture was stirred at 160 °C for 7 h. After the reaction was finished, the mixture was cooled to room temperature and extracted with ethyl acetate (3×20 mL), then the organic layer was washed with brine, and dried over anhydrous Na_2SO_4. The solvent was evaporated under reduced pressure, and the crude product was purified by column chromatography (silica gel, EA:DCM = 1:20) to give the yellow solid (122.0 mg, yield: 21%). ^{1}H NMR (400 MHz, DMSO-d_6): δ 8.71–8.65 (m, 4H), 6.99 (d, J = 8.5 Hz, 2H), 6.66 (d, 2H), 4.07–4.01 (m, 2H), 1.91–1.85 (m, 1H), 1.34–1.28 (m, 9H), 0.91–0.86 (m, 7H). HRMS (EI), *m/z*: $[M]^+$ calcd for $C_{28}H_{27}N_3O_4$: 469.2002; found: 469.1999.

Synthesis of 3. Under N_2 atmosphere, compound **1** (227.4 mg, 0.60 mmol) and 2,5-dimethyl-1,4-phenylenediamine (84.4 mg, 0.62 mmol) were dissolved in DMF (10 mL). The mixture was stirred at 160 °C for 7 h. After the reaction was finished, the mixture was cooled to room temperature and extracted with ethyl acetate (3×10 mL), then the organic layer was washed with brine, and dried over anhydrous Na_2SO_4. The solvent was evaporated under reduced pressure, and the crude product was

purified by column chromatography (silica gel, EA:DCM = 1:20) to give the yellow solid (178.9 mg, yield: 60%). ^{1}H NMR (400 MHz, $CDCl_3$): δ 8.82–8.78 (m, 4H), 6.88 (s, 1H), 6.69 (s, 1H), 4.22–4.12 (m, 2H), 2.17 (s, 3H), 2.04, (s, 3H), 1.99–1.93 (m, 1H), 1.43–1.31 (m, 9H), 0.97–0.87 (m, 7H). HRMS (EI), *m/z*: $[M]^+$ calcd for $C_{30}H_{31}N_3O_4$:497.2315; found: 497.2333.

Rho-NDI. FT-IR (KBr, cm^{-1}): 2965 (s; $\nu_{as}(CH_3)$), 2927 (s; $\nu_{as}(CH_2)$), 2871 (s; $\nu_s(CH_3)$), 2858 (s; $\nu_s(CH_2)$), 1713 (m; ν_{as}(C=O)), 1670 (m; ν_s(C=O)), 1615 (m; ν_{as}(Ar–C=C)), 1514 (m; ν_{as}(Ar–C=C)), 1449 (m; $\delta(CH_3)$), 1308 (m; ν_{as}(C–N)), 1242 (m; ν_s(C–N)), 1119 (m; ν_{as}(C–N)), 1080 (m; ν_s(C–N)), 1018 (m; ν_{as}(C–O–C)), 983 (m; ν_s(C–O–C)), 763 (s; ω(Ar–CH)).[3–5] Absorption band centered at 3440 cm^{-1} was assigned to the O–H of water in KBr.

Rho-Ph-NDI. FT-IR (KBr, cm^{-1}): 2963 (s; $\nu_{as}(CH_3)$), 2926 (s; $\nu_{as}(CH_2)$), 2870 (s; $\nu_s(CH_3)$), 2856 (s; $\nu_s(CH_2)$), 1707 (m; ν_{as}(C=O)), 1669 (m; ν_s(C=O)), 1615 (m; ν_{as}(Ar–C=C)), 1511 (m; ν_{as}(Ar–C=C)), 1451 (m; $\delta(CH_3)$), 1332 (m; ν_{as}(Ar–C–N)), 1247 (m; ν_s(Ar–C–N)), 1118 (m; ν_{as}(C–N)), 1093 (m; ν_s(C–N)), 1019 (m; ν_{as}(C–O–C)), 984 (m; ν_s(C–O–C)), 769 (s; ω(Ar–CH)).[3–5] Absorption band centered at 3440 cm^{-1} was assigned to the O–H of water in KBr.

Rho-PhMe-NDI. FT-IR (KBr, cm^{-1}): 2965 (s; $\nu_{as}(CH_3)$), 2928 (s; $\nu_{as}(CH_2)$), 2871 (s; $\nu_s(CH_3)$), 2859 (s; $\nu_s(CH_2)$), 1707 (m; ν_{as}(C=O)), 1670 (m; ν_s(C=O)), 1614 (m; ν_{as}(Ar–C=C)), 1513 (m; ν_{as}(Ar–C=C)), 1451 (m; $\delta(CH_3)$), 1331 (m; ν_{as}(Ar–C–N)), 1247 (m; ν_s(Ar–C–N)), 1119 (m; ν_{as}(C–N)), 1093 (m; ν_s(C–N)), 1018 (m; ν_{as}(C–O–C)), 984 (m; ν_s(C–O–C)), 771 (s; ω(Ar–CH)).[3–5] Absorption band centered at 3440 cm^{-1} was assigned to the O–H of water in KBr.

2. Molecular Structure Characterization Data

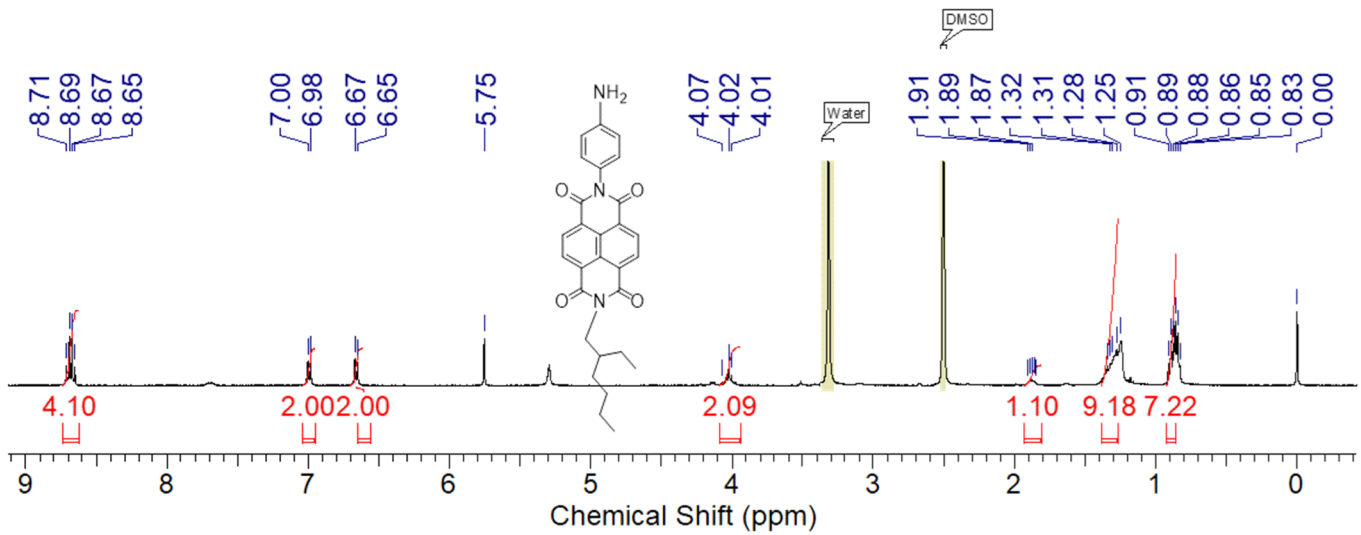

Fig. S1 ^{1}H NMR spectrum of **2** (400 MHz, DMSO-d_6).

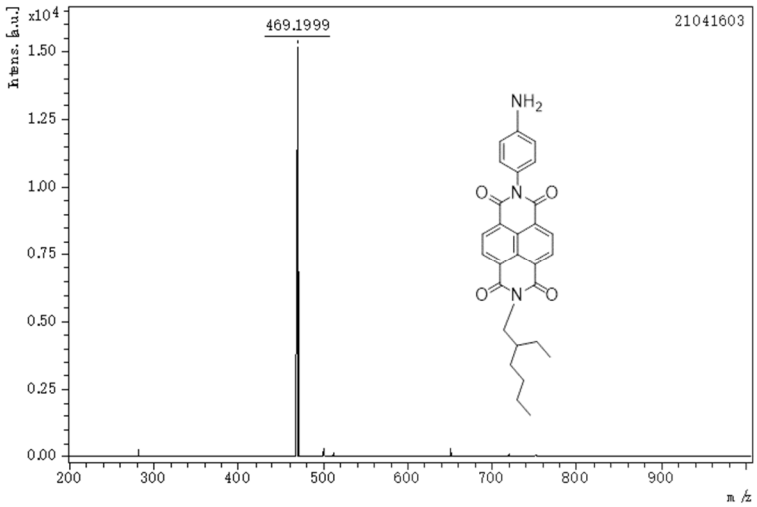

Fig. S2 EI-TOF mass spectrum of **2**.

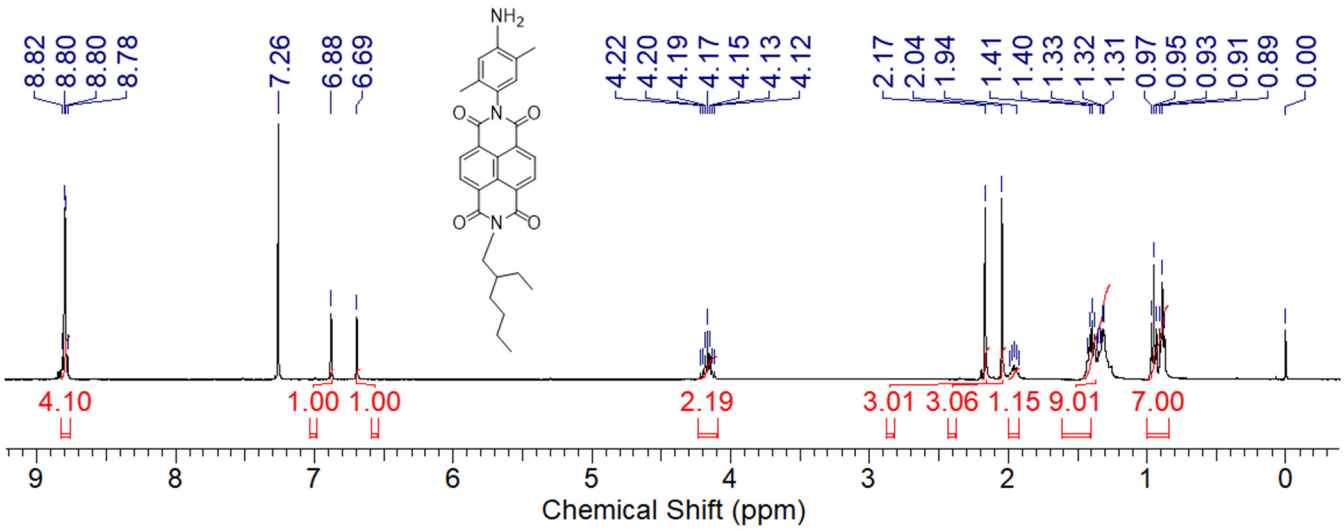

Fig. S3 ^{1}H NMR spectrum of **3** (400 MHz, $CDCl_3$).

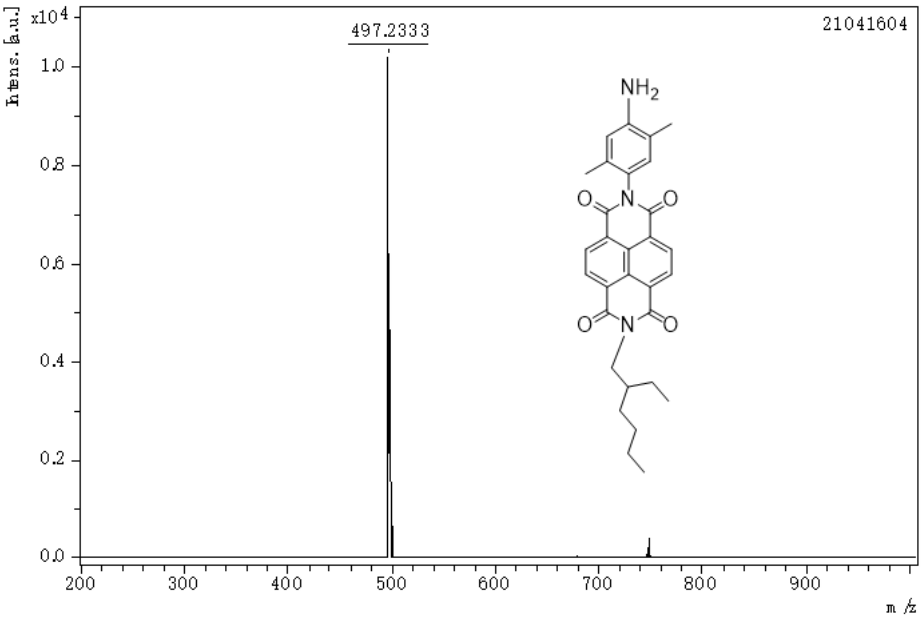

Fig. S4 EI-TOF mass spectrum of **3**.

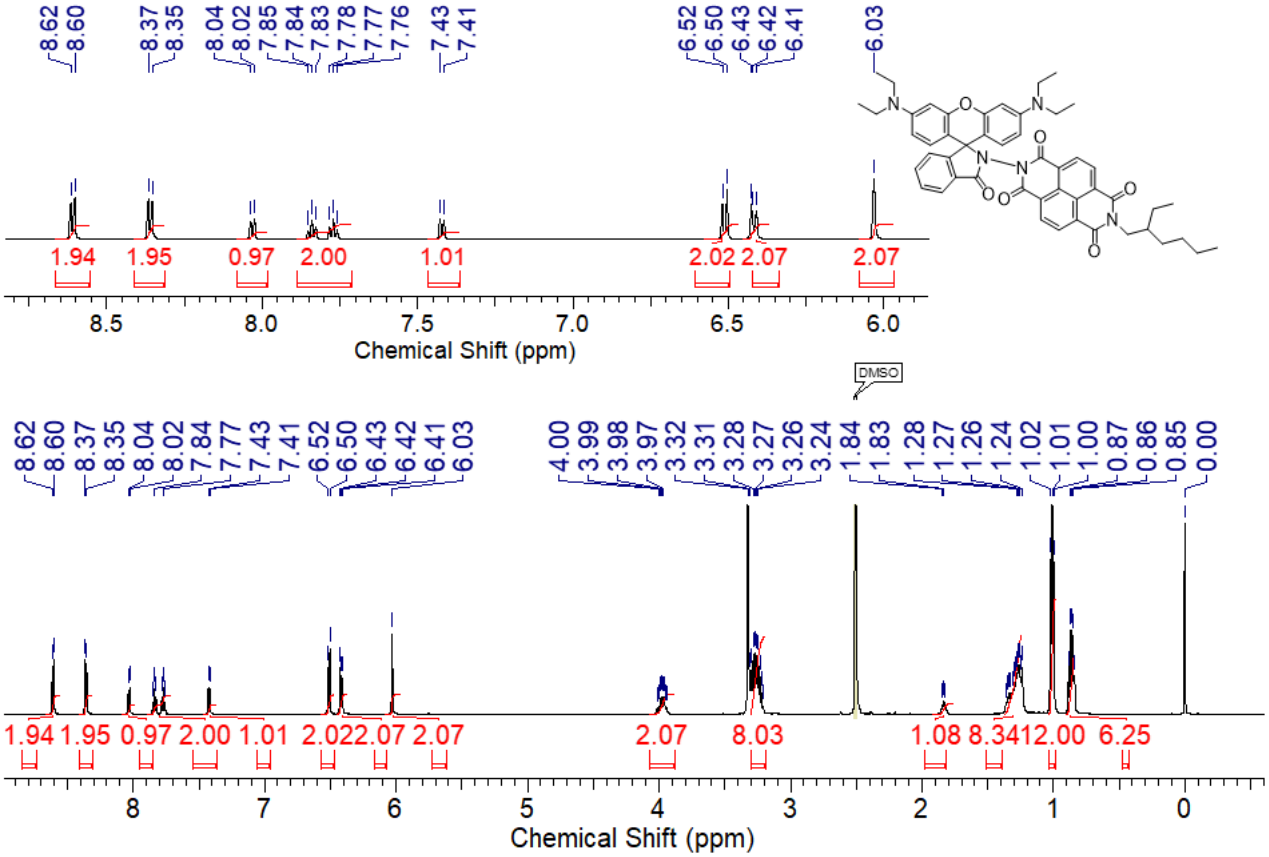

Fig. S5 ^{1}H NMR spectra of **Rho-NDI** (600 MHz, DMSO-d_6).

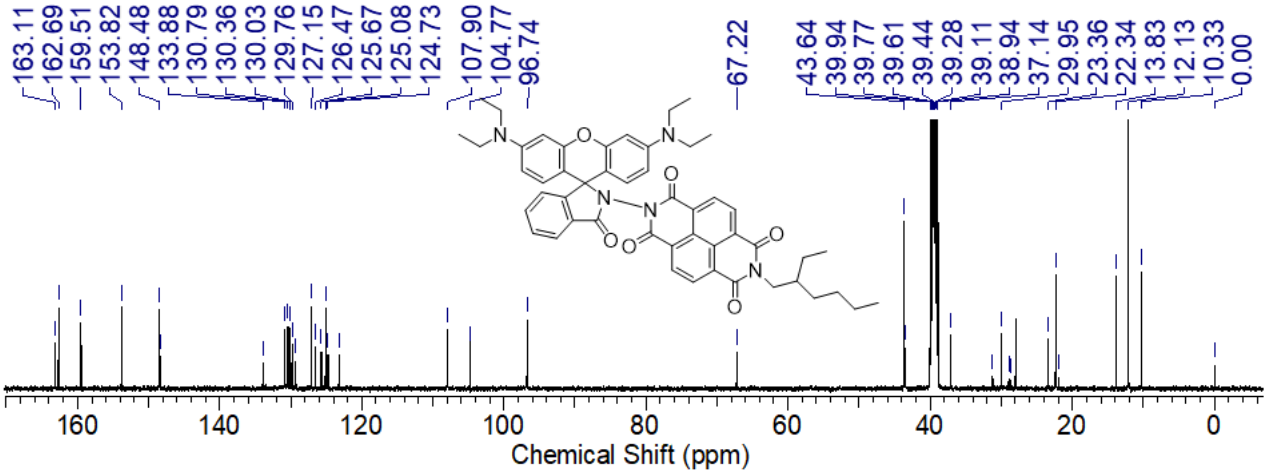

Fig. S6 ^{13}C NMR spectrum of **Rho-NDI** (125 MHz, DMSO-d_6).

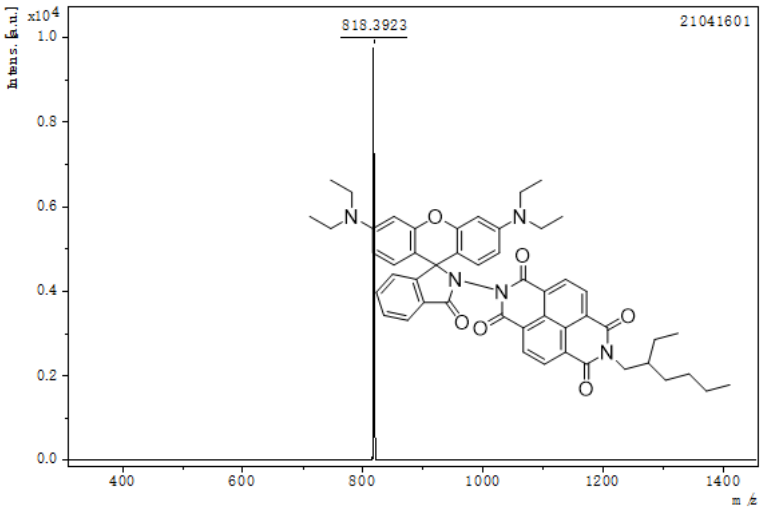

Fig. S7 EI-TOF mass spectrum of **Rho-NDI**.

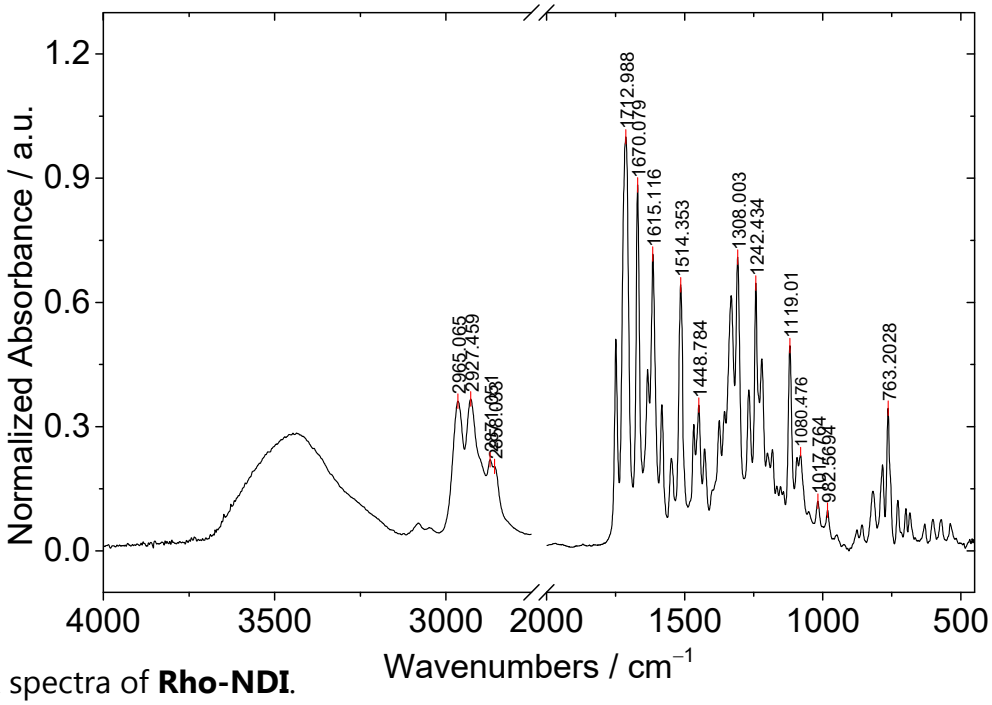

Fig. S8 FT-IR spectra of **Rho-NDI**.

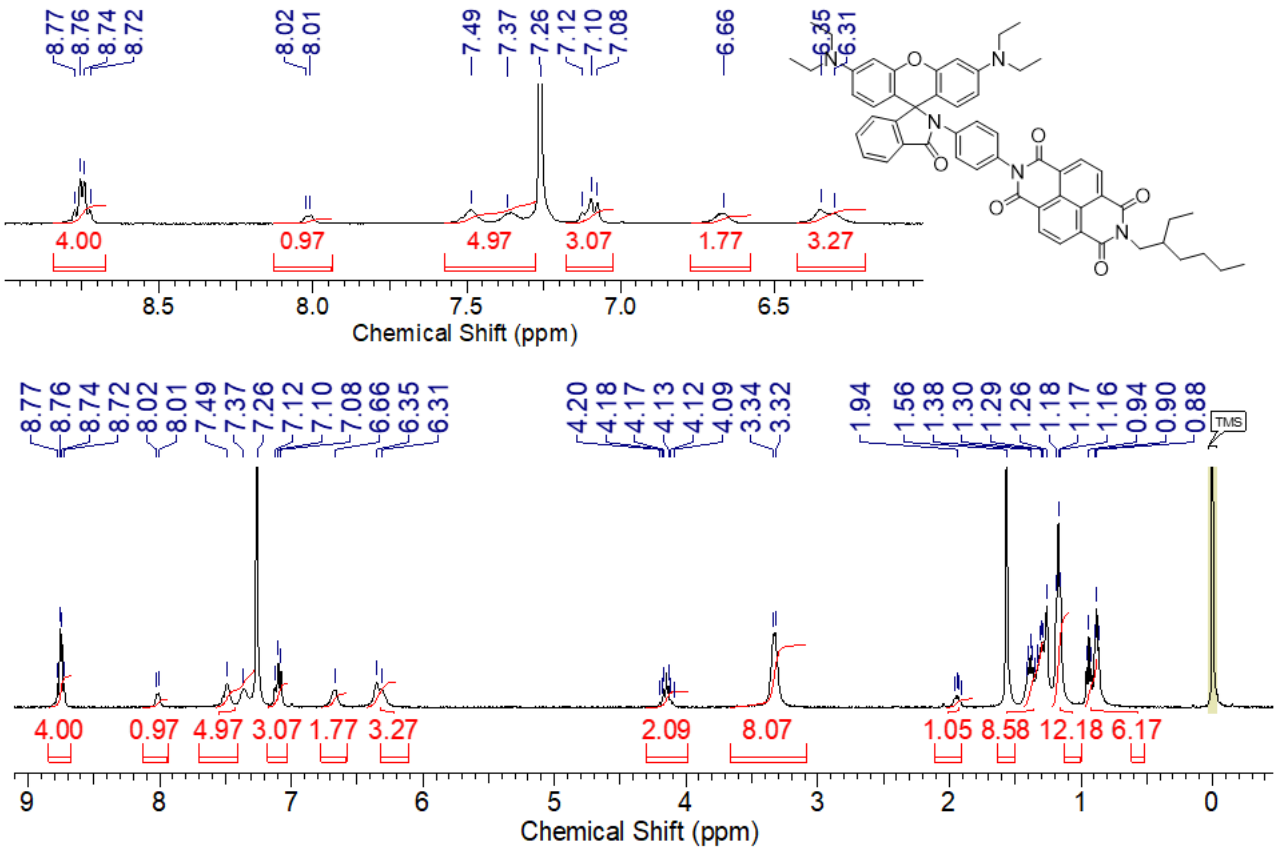

Fig. S9 ^{1}H NMR spectra of **Rho-Ph-NDI** (600 MHz, $CDCl_3$).

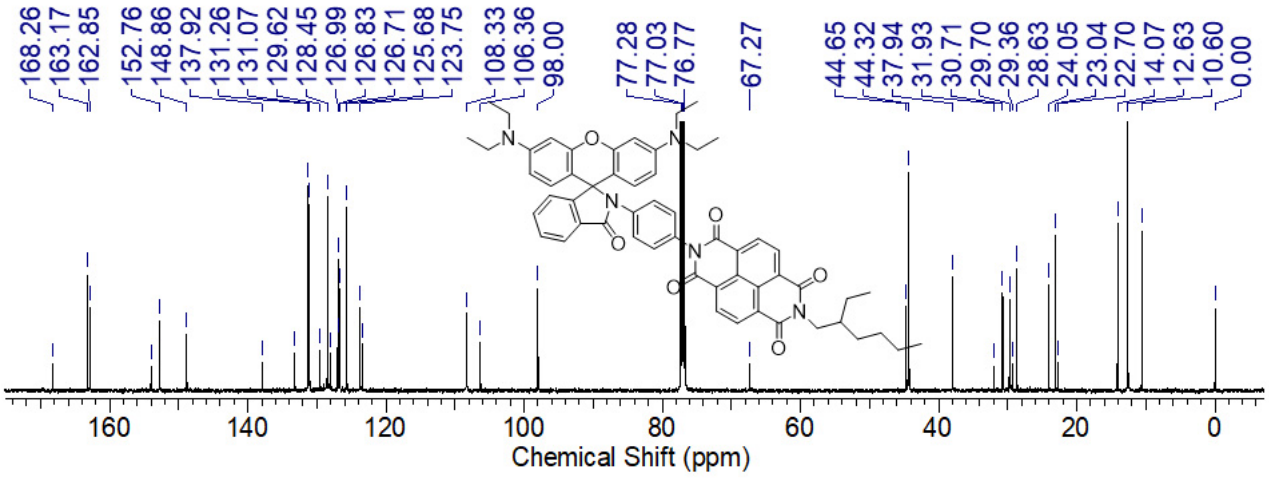

Fig. S10 ^{13}C NMR spectrum of **Rho-Ph-NDI** (125 MHz, $CDCl_3$).

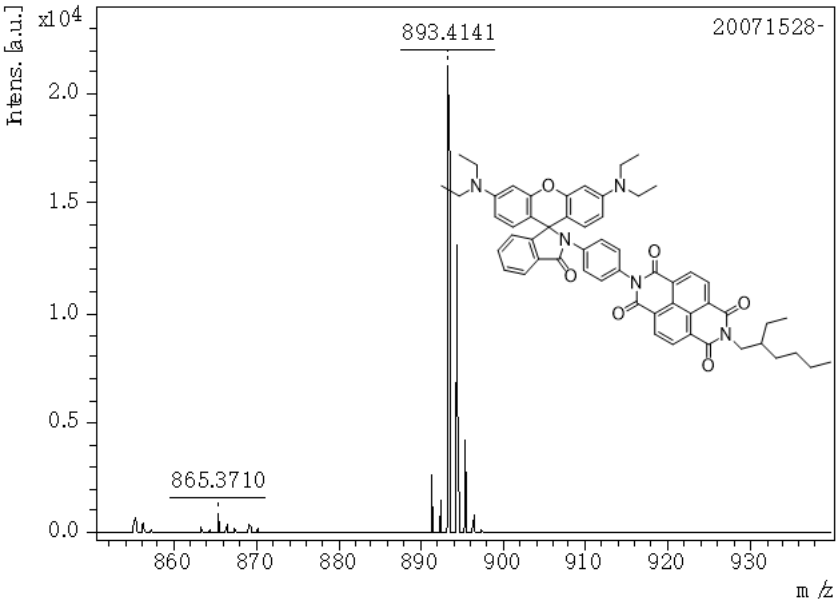

Fig. S11 EI-TOF mass spectrum of **Rho-Ph-NDI**.

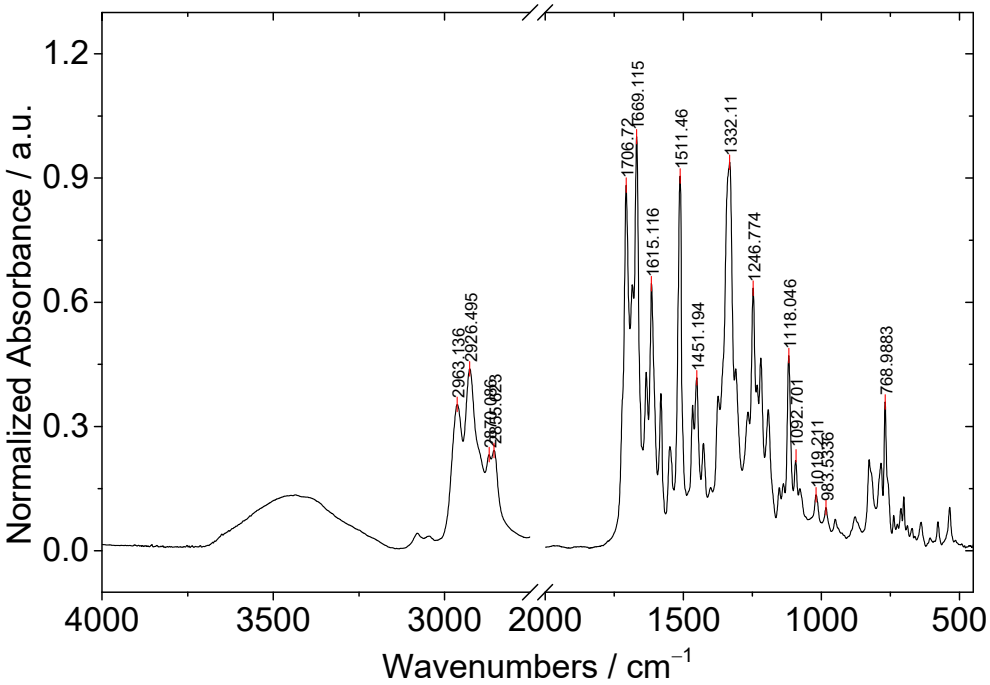

Fig. S12 FT-IR spectra of **Rho-Ph-NDI**.

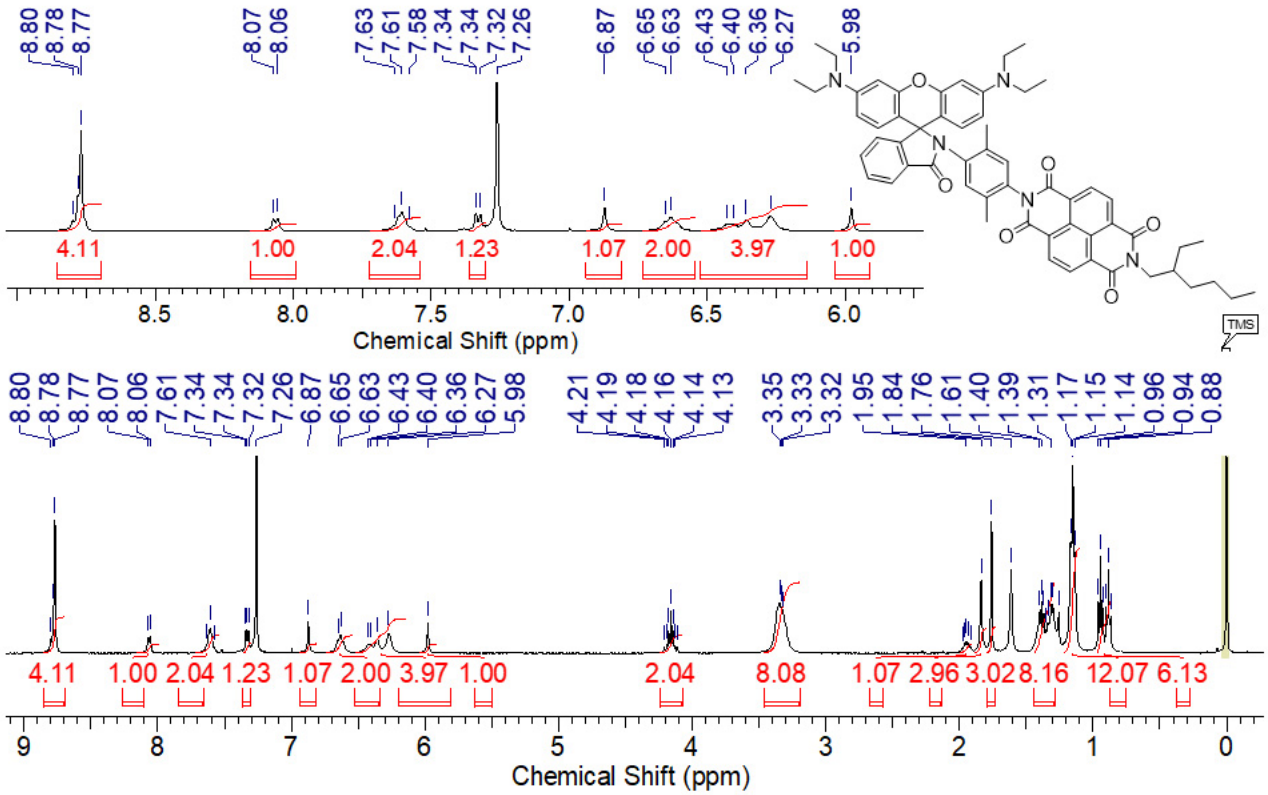

Fig. S13 ^{1}H NMR spectra of **Rho-PhMe-NDI** (600 MHz, $CDCl_3$).

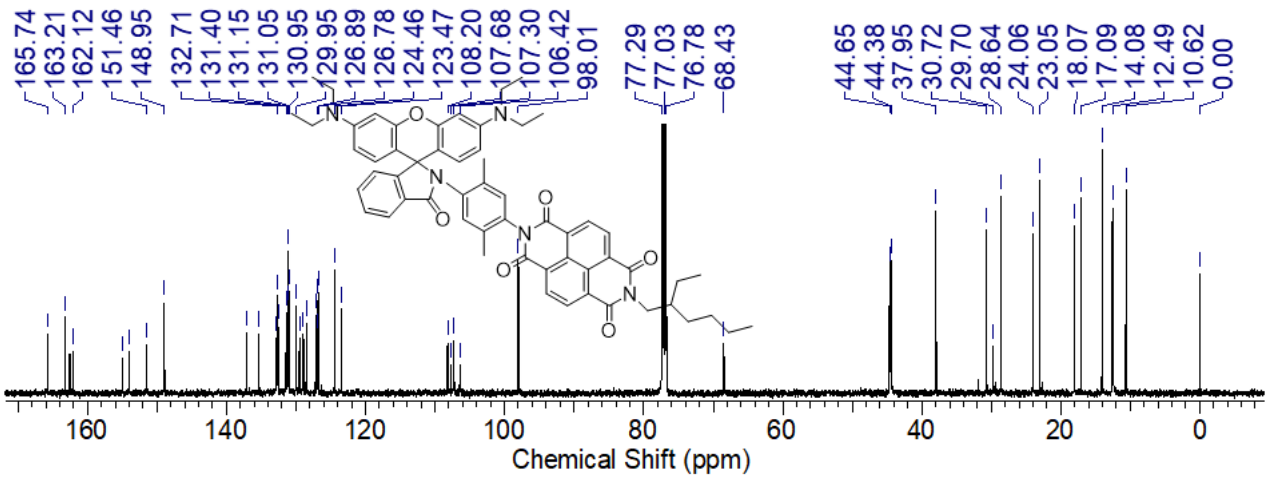

Fig. S14 ^{13}C NMR spectrum of **Rho-PhMe-NDI** (125 MHz, $CDCl_3$).

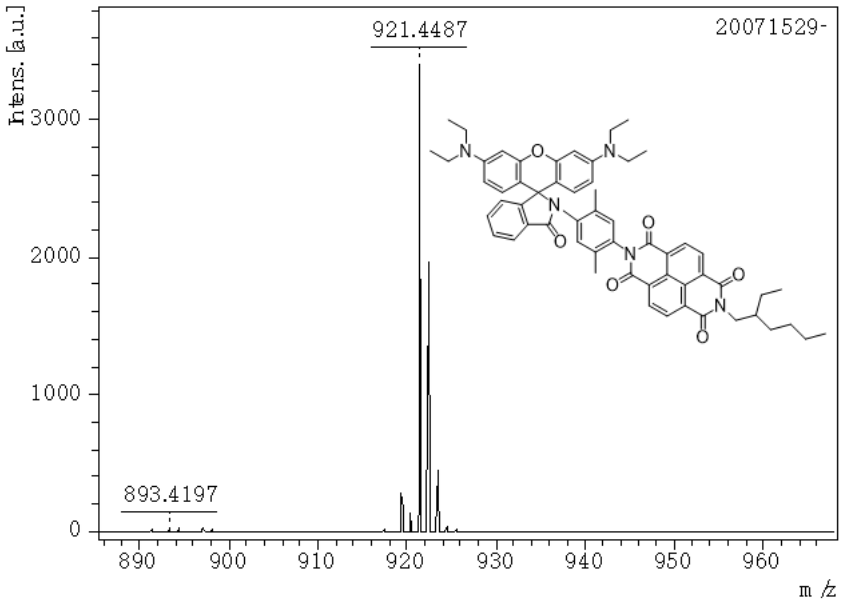

Fig. S15 EI-TOF mass spectrum of **Rho-PhMe-NDI**.

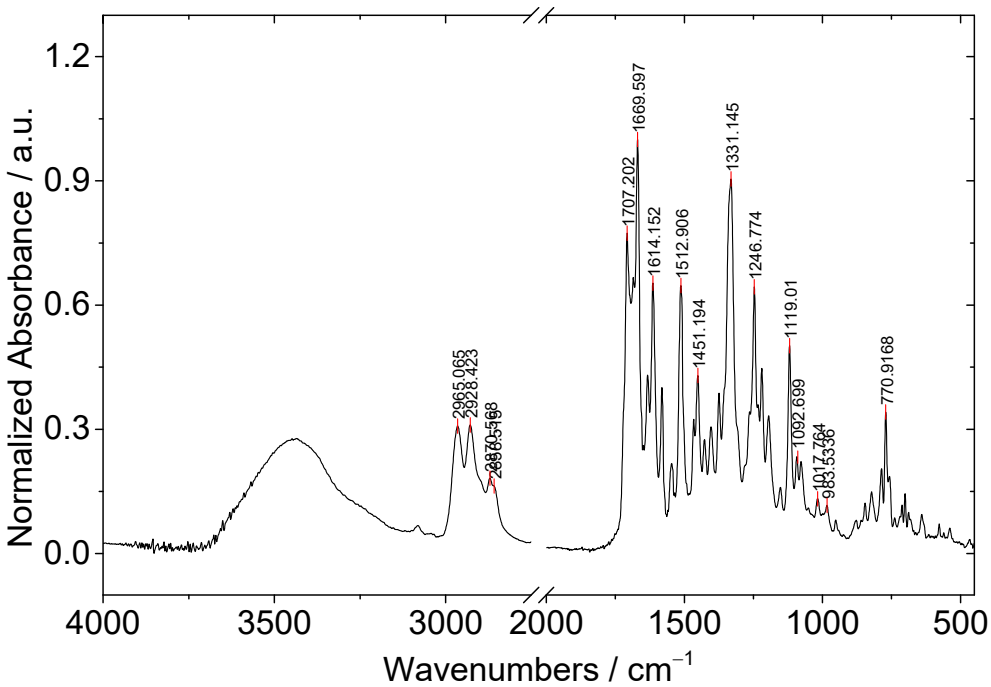

Fig. S16 FT-IR spectra of **Rho-PhMe-NDI**.

3. Crystallographic data

Table S1 Crystallographic data of **Rho-NDI** (CCDC number: 2190442)

Compound	**Rho-NDI**
Empirical formula	$C_{45}H_{41}N_5O_6$
Formula weight	747.86
Colour	red
Temperature (K)	120
Wavelength (Å)	0.71073
Crystal system	triclinic
Space group	P-1
a (Å)	9.7228
b (Å)	12.0523
c (Å)	16.1605
α (deg)	74.238
β (deg)	88.581
γ (deg)	86.213
Volume (Å^3)	1818.49
Z	2
Dx / g·cm^{-3}	1.366
F (000)	788.4
μ / mm^{-1}	0.092
Data completeness	0.995
Absorption correction	None
Goodness of fit on F^2	1.064
R	0.0426
ωR_2	0.1134

4. Steady State UV–vis Absorption Spectra

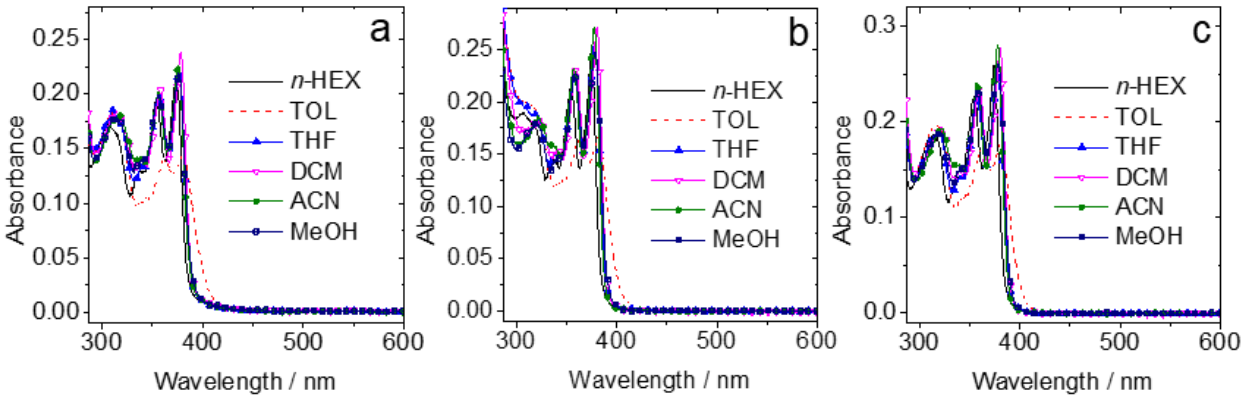

Fig. S17 UV–Vis absorption spectra of (a) **Rho-NDI**, (b) **Rho-Ph-NDI** and (c) **Rho-PhMe-NDI** in different solvents. c = 1.0 × 10^{-5} M, 25 °C.

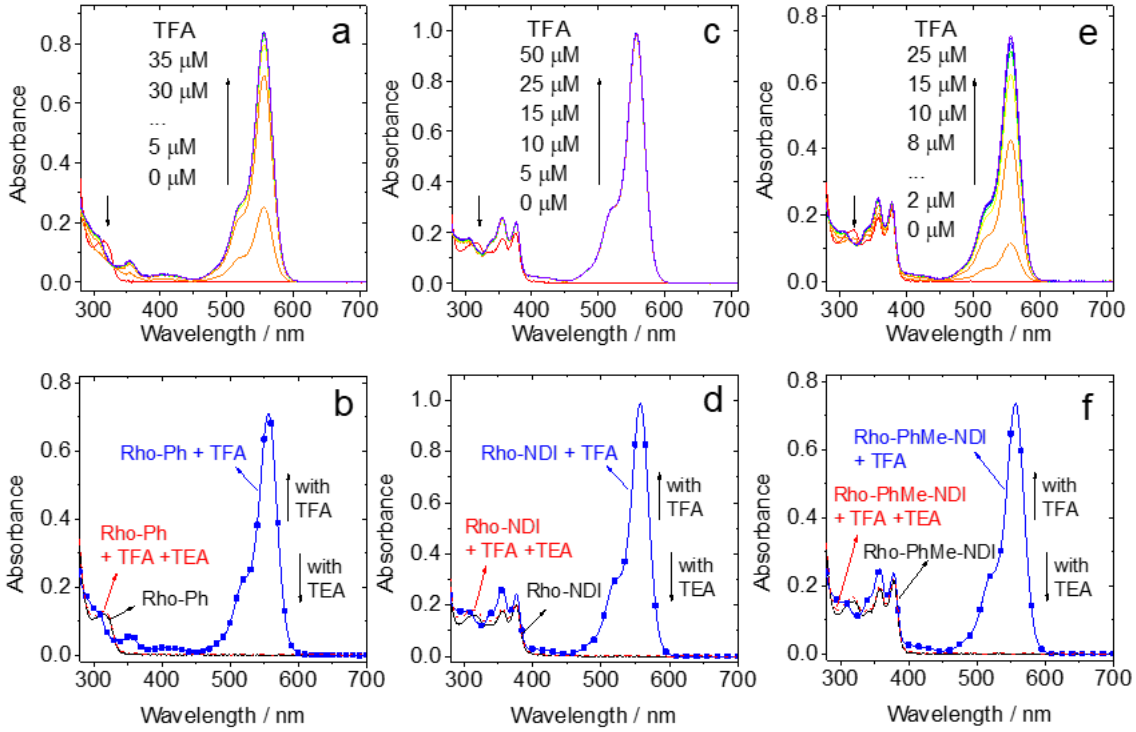

Fig. S18 UV−vis absorption spectra of (a) Rho-Ph, (c) **Rho-NDI** and (e) **Rho-PhMe-NDI** with gradual addition of TFA. And UV−vis absorption spectra of (b) Rho-Ph, (d) **Rho-NDI** and (f) **Rho-PhMe-NDI** with addition of TFA (c = 50 μM) or TEA (neat, 10 μL) in MeOH. c = 1.0 × 10^{-5} M. 25 °C.

5. Fluorescence Spectra and Fluorescence Lifetimes

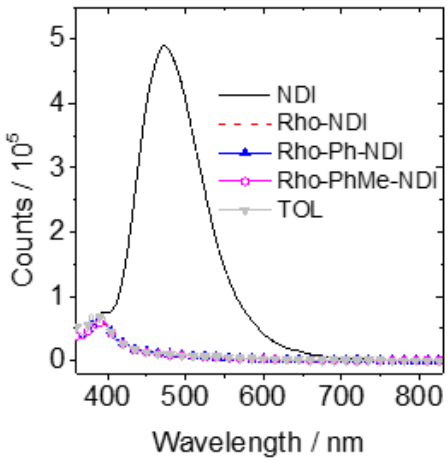

Fig. S19 Fluorescence emission spectra of the compounds in TOL. Optically matched solutions were used (λ_{ex} = 320 nm, A = 0.1). 25 °C.

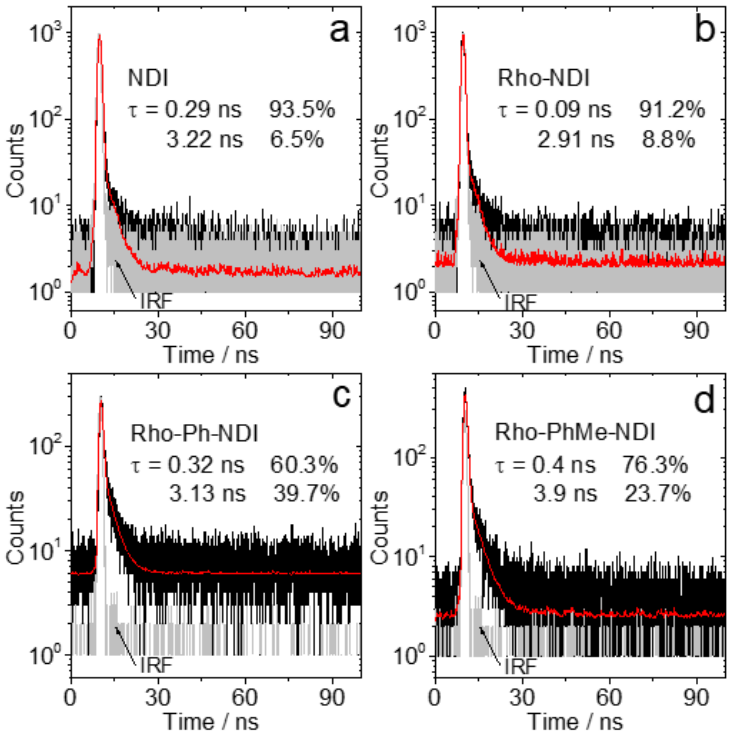

Fig. S20 Fluorescence decay traces of (a) **NDI** at 420 nm, (b)**Rho-NDI** at 710 nm, (c) **Rho-Ph-NDI** at 750 nm and (d) **Rho-PhMe-NDI** at 750 nm in HEX. λ_{ex} = 340 nm, c = 1.0 × 10^{-5} M, 25 °C.

6. Electrochemical Studies

For the eqs 2-5, where ΔG_S is the static Coulombic energy, ΔG_{CS}^0 is the Gibbs free-energy change of charge separation process ΔG_{CR}^0 is the Gibbs free-energy change of charge recombination process and E_{CSS} is the energy levels of the charge separated state. e is the electronic charge, E_{OX} is the half-wave potential for one-electron oxidation of the electron-donor unit, E_{RED} is the half-wave potential for one-electron reduction of the electron-acceptor unit, E_{00} is the approximated energy UV−Vis absorption at the singlet excited state in HEX, ε_S is the static dielectric constant of the solvent, R_{CC} is the center-to-center separation distance between the electron donor (rhodamine) and electron acceptor (naphthalenediimide), determined by DFT optimization of the geometry, R_{CC} (**Rho-NDI**) = 6.01 Å, R_{CC} (**Rho-Ph-NDI**) = 10.08 Å, R_{CC} (**Rho-PhMe-NDI**) = 9.94 Å, R_D is the radius of the electron donor, R_A is the radius of the electron acceptor, ε_{REF} is the static dielectric constant of the solvent used for the electrochemical studies, ε_0 is permittivity of free space. The solvents used in the calculation of free energy of the electron transfer is HEX (ε_S = 1.88), TOL (ε_S = 2.38), THF (ε_S = 7.39), DCM (ε_S = 8.93) and ACN (ε_S = 37.5).

7. Chemical Redox and Spectroelectrochemistry Study

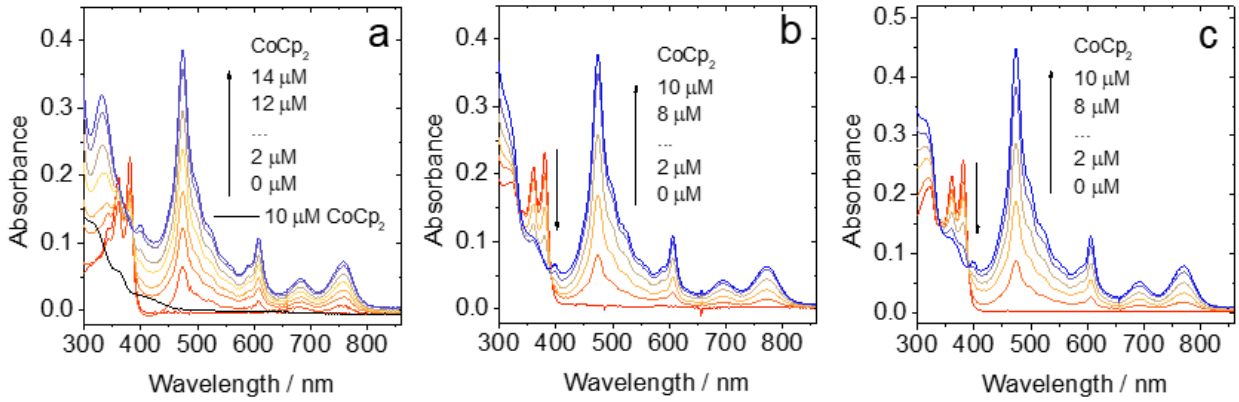

Fig. S21 UV–vis absorption spectra of (a) **NDI**, (b) **Rho-Ph-NDI** and (c) **Rho-PhMe-NDI** chemically reduced with cobaltocene ($CoCp_2$) used to generate $NDI^{-\bullet}$ in deaerated *N,N*-dimethylformamide. $c = 1.0 \times 10^{-5}$ M, 25 °C.

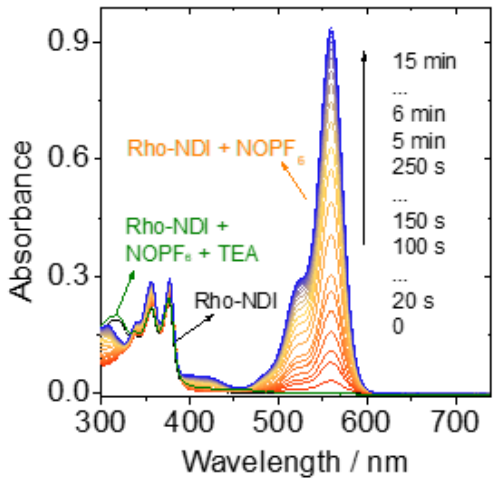

Fig. S22 The change of the UV–vis absorption spectra of **Rho-NDI** with time chemically oxidized with $NOPF_6$, then with the addition of TEA in deaerated ACN. c[**Rho-NDI**] = 1.0×10^{-5} M, 25 °C.

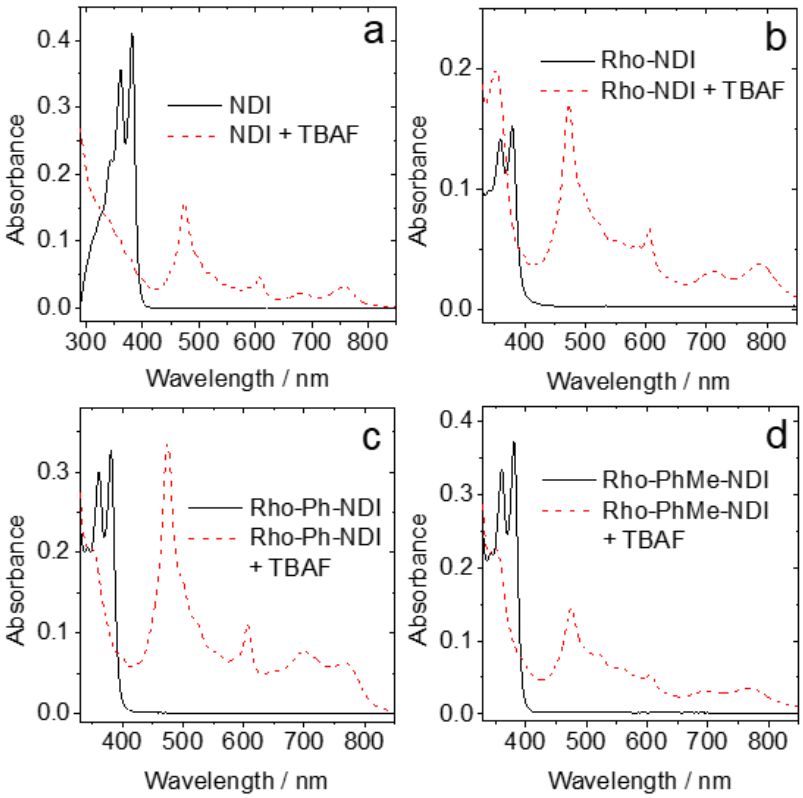

Fig. S23 UV–vis absorption spectra of (a) **NDI**, (b) **Rho-NDI**, (c) **Rho-Ph-NDI** and (d) **Rho-PhMe-NDI** chemically reduced with tetrabutylammonium fluoride (TBAF) used to generate $NDI^{-\bullet}$ in deaerated *N,N*-dimethylformamide. *c*[Sample] = 1.0 × 10^{-5} M, *c*[TBAF] = 5.0 × 10^{-3} M, 25 °C.

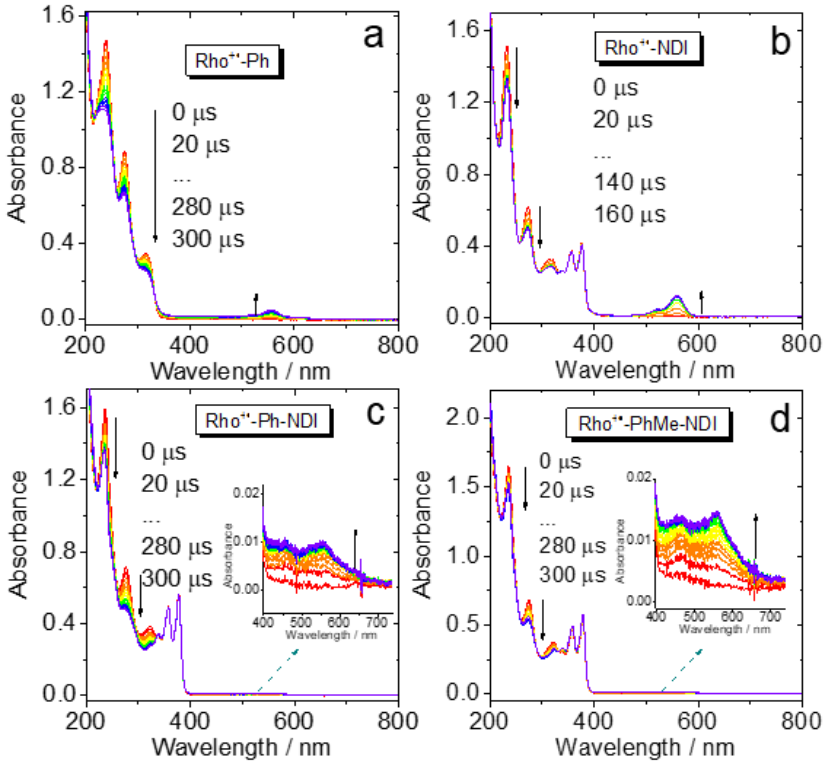

Fig. S24 The UV–vis absorption changes of (a) **Rho-Ph**, (b) **Rho-NDI**, (c) **Rho-Ph-NDI** and (b) **Rho-PhMe-NDI** upon oxidation under 0.63 V in deaerated ACN. The spectra were recorded in situ with a spectroelectrochemical cuvette (1 mm optical path). *c*[Sample] = ca. 2.5 × 10^{-4} M. 25 °C.

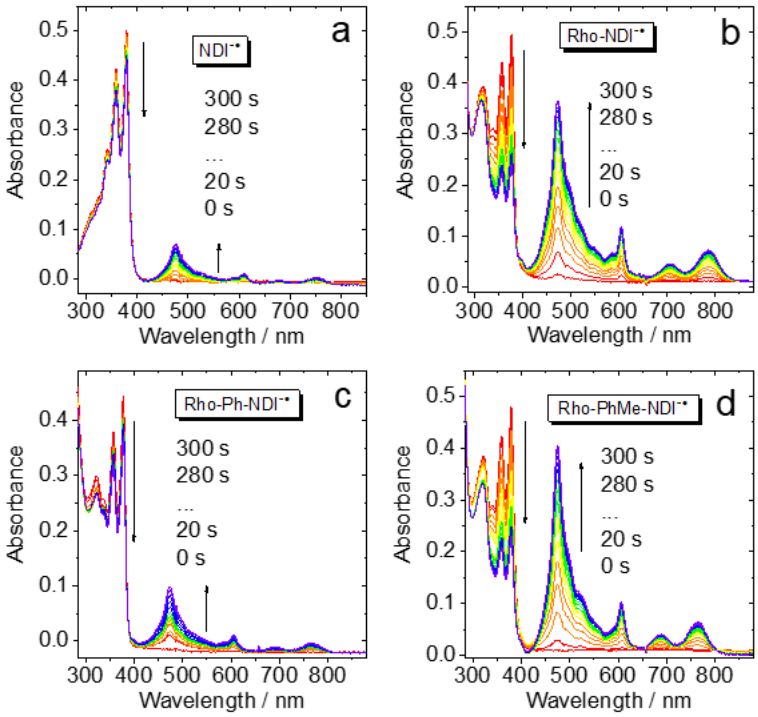

Fig. S25 The spectroelectrochemistry study of (a) **NDI**, (b) **Rho-NDI**, (c) **Rho-Ph-NDI** and (c) **Rho-PhMe-NDI** by monitoring the evolution of UV–vis absorption upon a potential of –1.2 V (vs. $Ag/AgNO_3$) applied in deaerated ACN. The spectra were recorded in situ with a spectroelectrochemical cuvette (1 mm optical path). $c = 3.0 \times 10^{-4}$ M. 25 °C.

8. Femtosecond Transient Absorption Spectroscopy

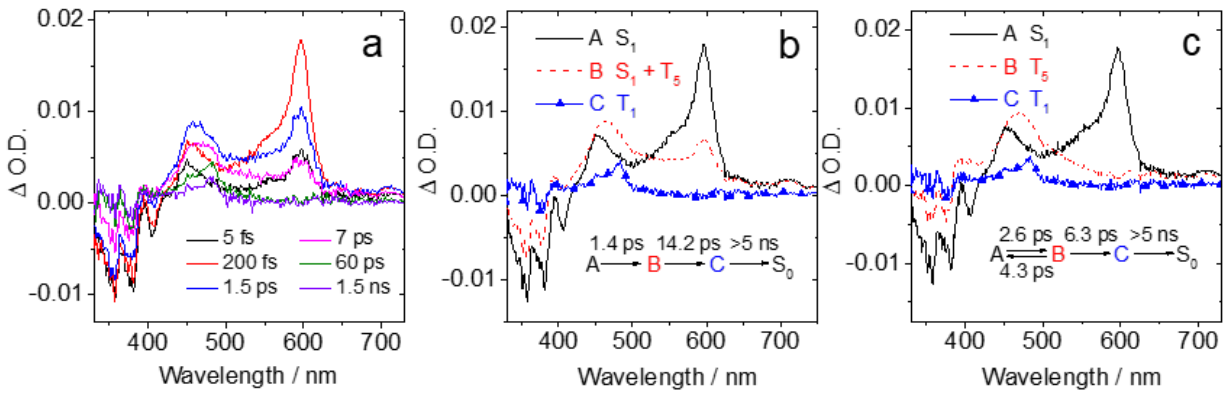

Fig. S26 (a) Femtosecond transient absorption spectra of **NDI** in acentronitrile. (b), (c) The related species-associated difference spectrum (SADS) obtained from target analysis assuming the reaction scheme in the inset. λ_{ex} = 375 nm. c = 1.0 × 10^{-4} M, 25 °C.

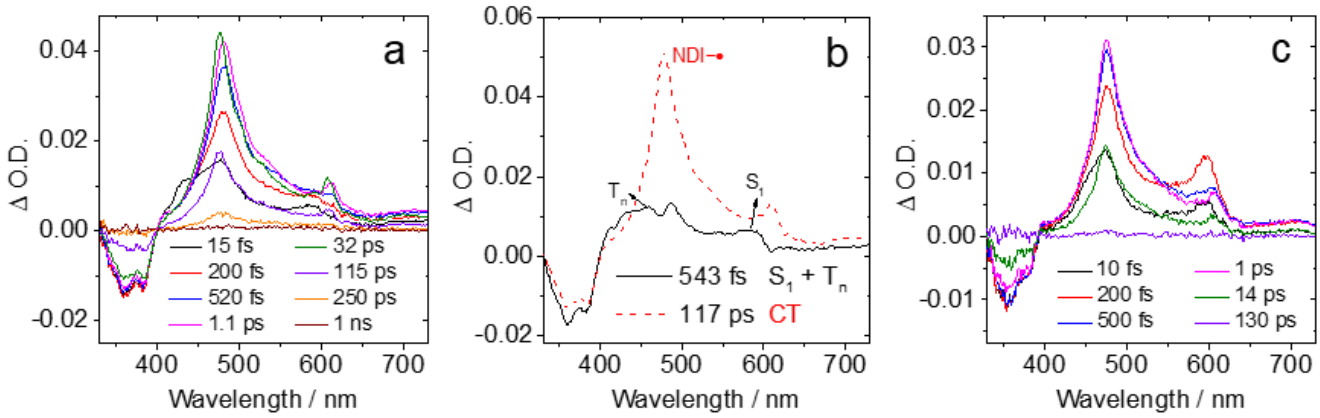

Fig. S27 Femtosecond transient absorption spectra of **Rho-NDI** (a) in TOL and (c) ACN. (b) The related species-associated difference spectrum (SADS) obtained from target analysis with sequential model in TOL. λ_{ex} = 375 nm. c = 1.0 × 10^{-4} M, 25 °C.

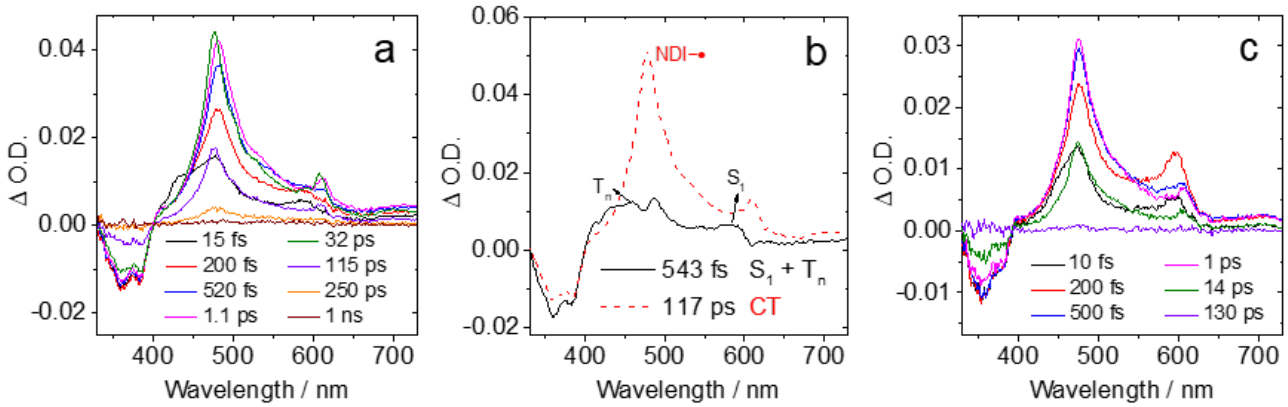

Fig. S28 Femtosecond transient absorption spectra of **Rho-Ph-NDI** (a) in TOL and (c) ACN. (b) The related species-associated difference spectrum (SADS) obtained from target analysis with sequential model in TOL. λ_{ex} = 375 nm. c = 1.0 × 10^{-4} M, 25 °C.

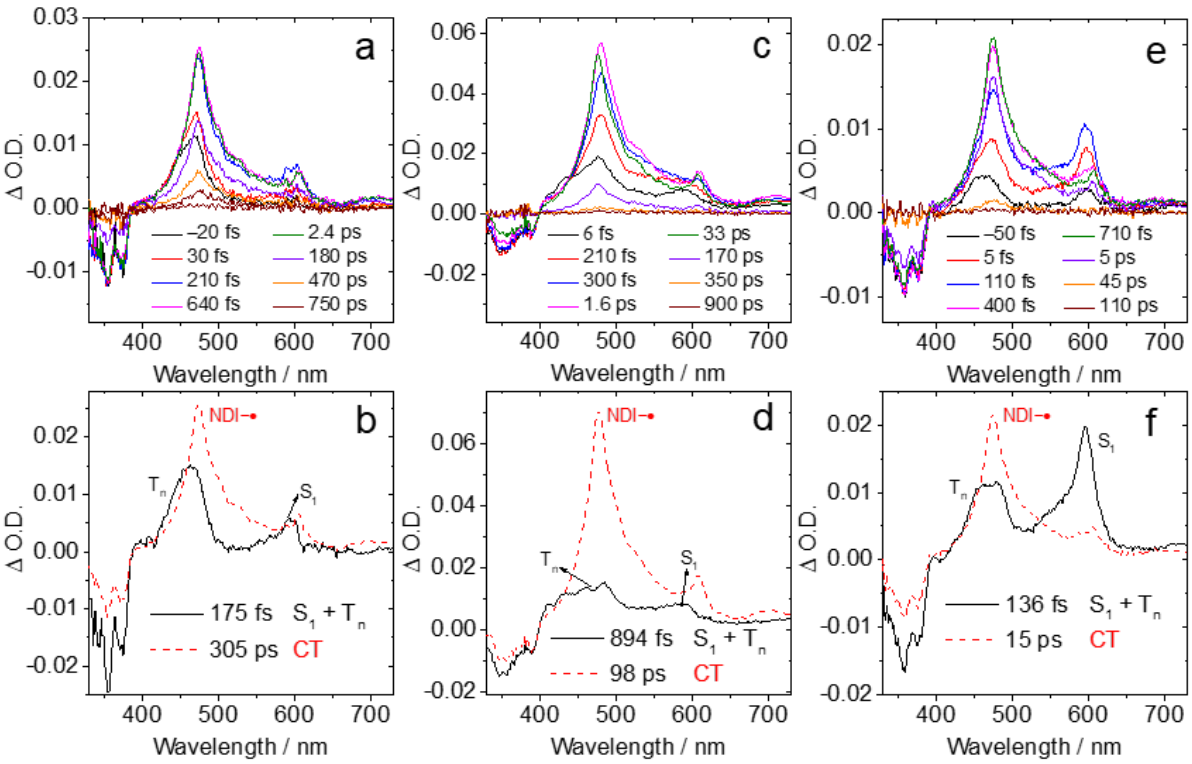

Fig. S29 Femtosecond transient absorption spectra of **Rho-PhMe-NDI** in (a) HEX, (c) TOL and (e) ACN. The related species-associated difference spectrum (SADS) obtained from target analysis with sequential model in (b) HEX, (d) TOL and (f) ACN. λ_{ex} = 375 nm. c = 1.0 × 10^{-4} M, 25 °C.

9. Nanosecond Transient Absorption Spectroscopy

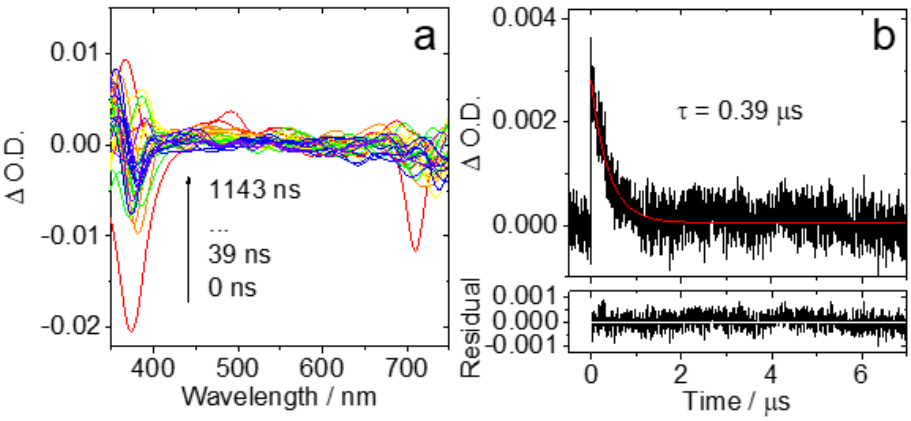

Fig. S30 (a) Nanosecond transient absorption spectra of **Rho-NDI** and (b) the decay trace in deaerated TOL at 470 nm excited with nanosecond pulsed laser. λ_{ex} = 355 nm. c = 1.0 × 10^{-4} M, 25 °C.

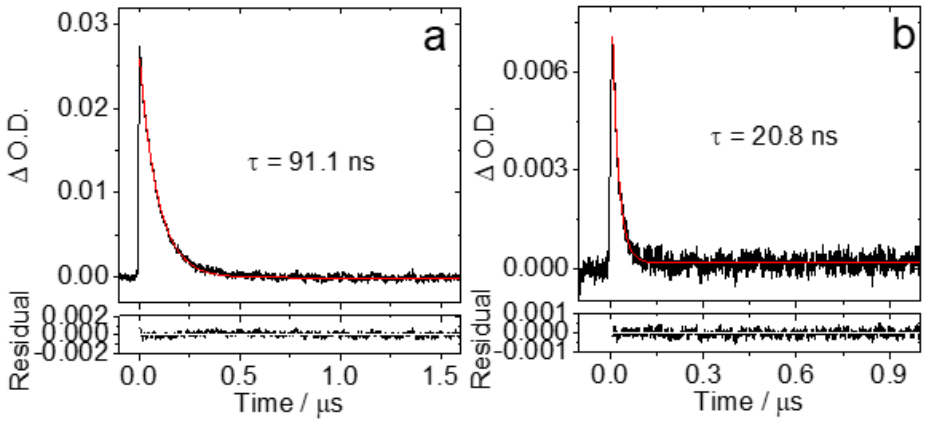

Fig. S31 The decay traces of **Rho-NDI** in aerated (a) HEX at 480 nm and (b) ACN at 470 nm excited with nanosecond pulsed laser**.** λ_{ex} = 355 nm. c = 3.0 × 10^{-5} M, 25 °C.

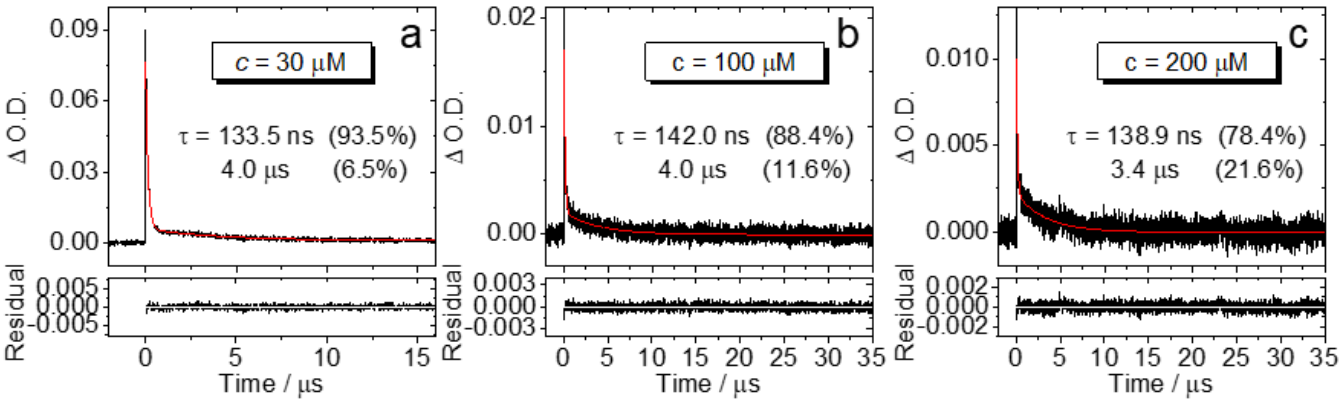

Fig. S32 The decay traces of **Rho-NDI** in deaerated HEX at 480 nm excited with nanosecond pulsed laser with different concentration. (a) c = 3.0 × 10^{-5} M, (b) c = 1.0 × 10^{-4} M and (c) c = 2.0 × 10^{-4} M. λ_{ex} = 355 nm, 25 °C.

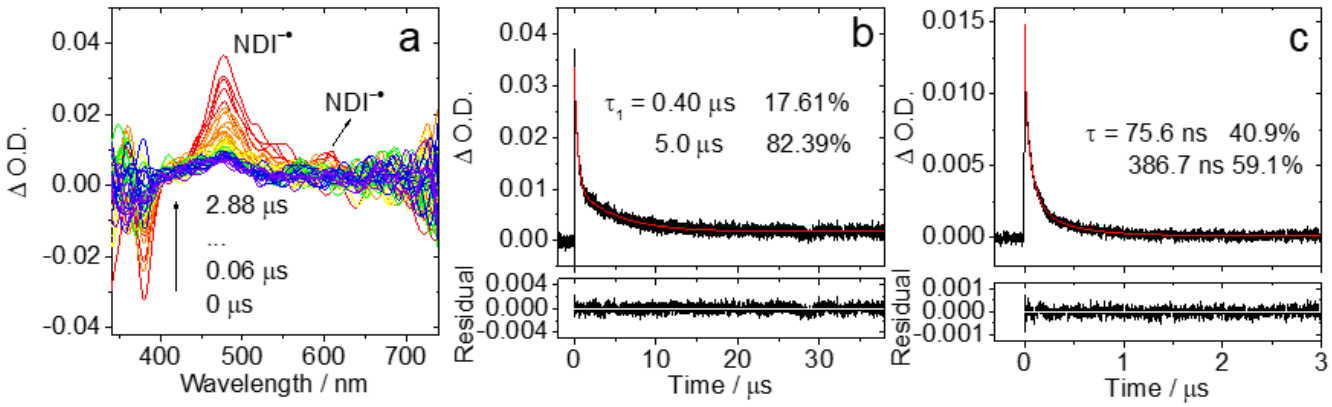

Fig. S33 (a) Nanosecond transient absorption spectra of **Rho-Ph-NDI** and the decay traces in (b) deaerated and (c) aerated TOL at 470 nm excited with nanosecond pulsed laser**.** λ_{ex} = 355 nm. c = 3.0 × 10^{-5} M, 25 °C.

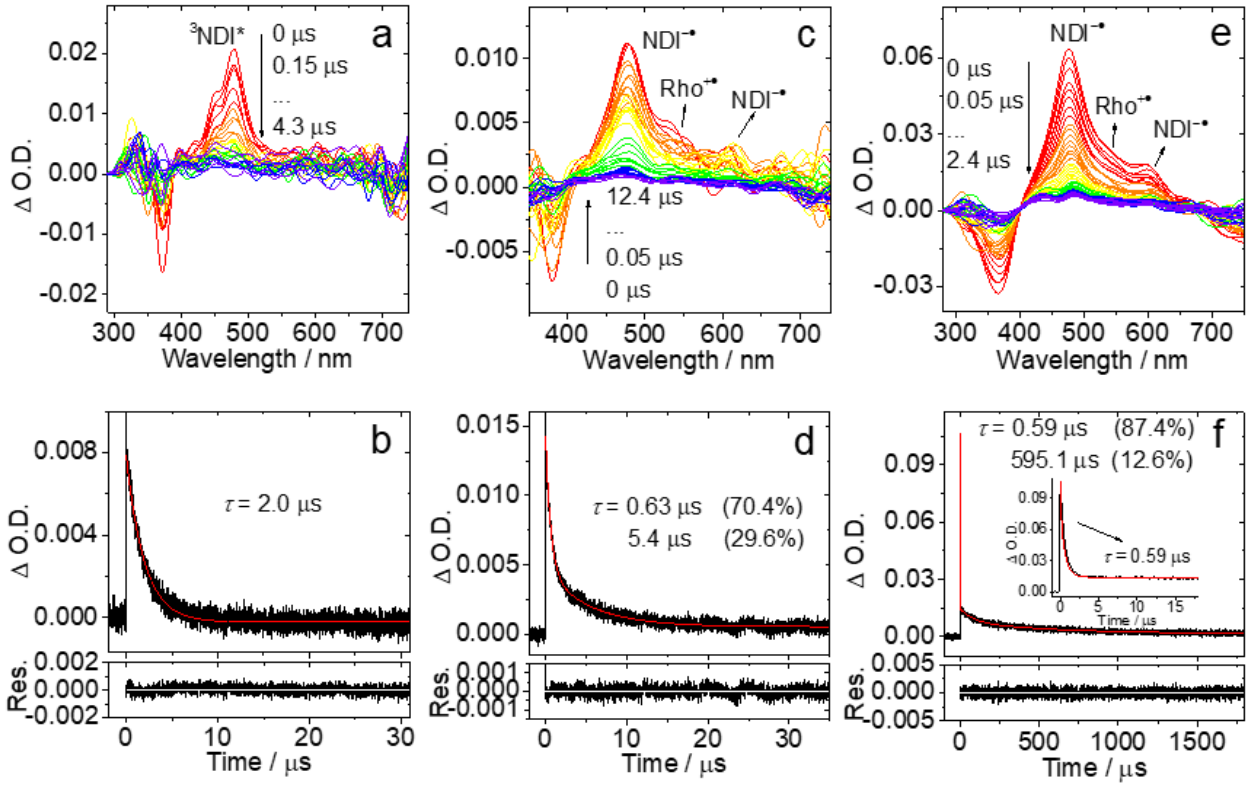

Fig. S34 Nanosecond transient absorption spectra of **Rho-PhMe-NDI** in deaerated (a) HEX, (c) TOL and (e) ACN. The decay traces of **Rho-PhMe-NDI** in deaerated (b) HEX at 485 nm, (d) TOL and (f) ACN at 470 nm. Excited with nanosecond pulsed laser. λ_{ex} = 355 nm. c = 3.0 × 10^{-5} M in HEX, c = 5.0 × 10^{-5} M in TOL and ACN, 25 °C.

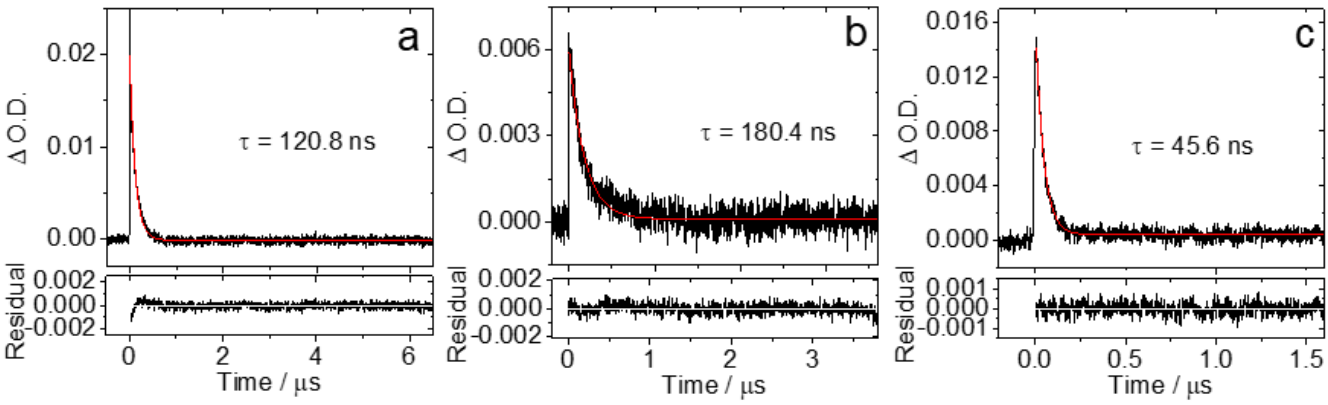

Fig. S35 The decay traces of **Rho-Ph-NDI** in aerated (a) HEX at 480 nm, (b) TOL and (c) ACN at 470 nm excited with nanosecond pulsed laser. λ_{ex} = 355 nm. c = 3.0 × 10^{-5} M in HEX and ACN, c = 5.0 × 10^{-5} M in TOL, 25 °C.

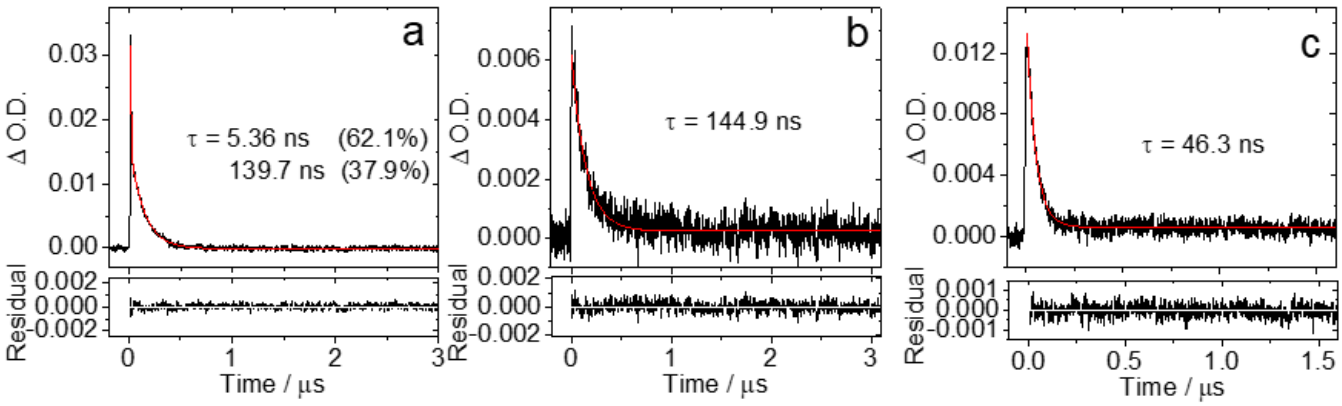

Fig. S36 The decay traces of **Rho-PhMe-NDI** in aerated (a) HEX at 480 nm, (b) TOL and (c) ACN at 470 nm excited with nanosecond pulsed laser. λ_{ex} = 355 nm. c = 3.0 × 10^{-5} M in HEX and TOL, c = 5.0 × 10^{-5} M in ACN, 25 °C.

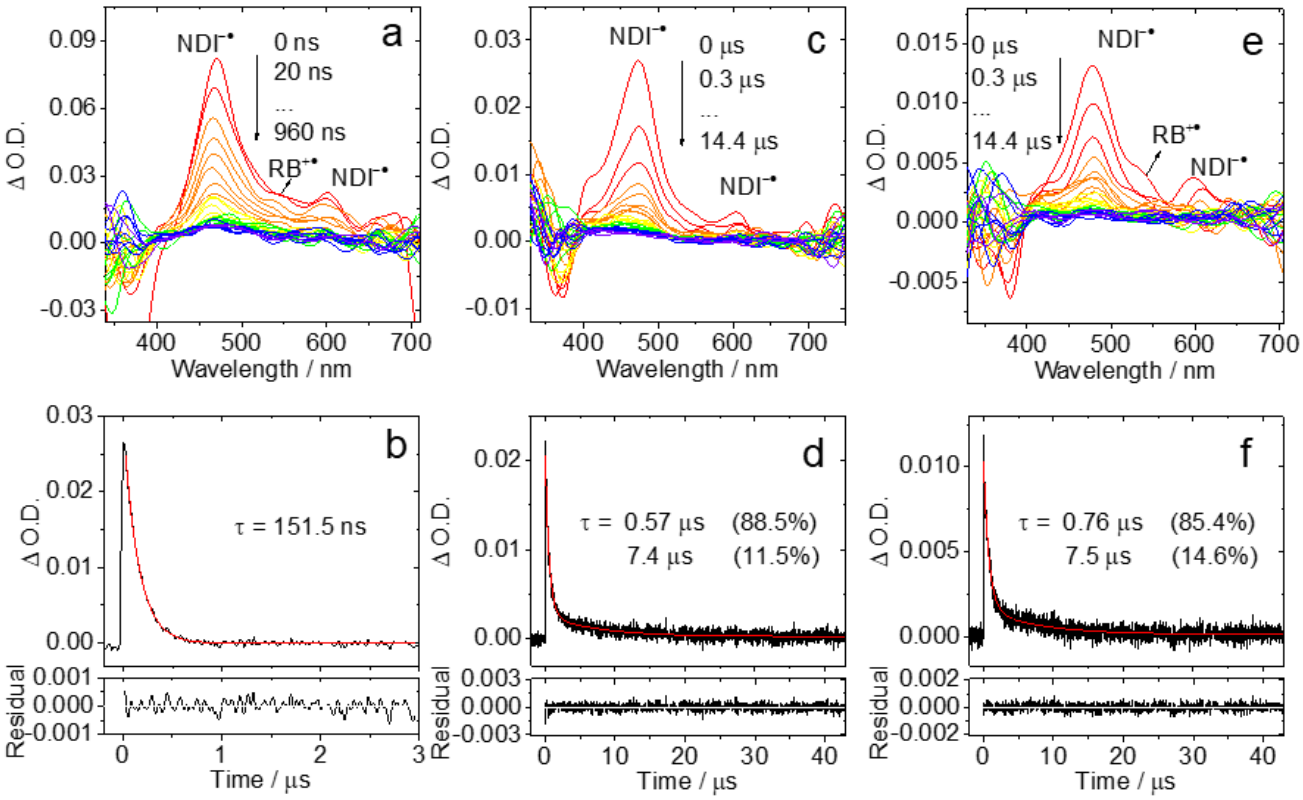

Fig. S37 Nanosecond transient absorption spectra of (a) **Rho-NDI**, (c) **Rho-Ph-NDI** and (e) **Rho-PhMe-NDI** in deaerated viscous solvent dimethylsilicone oil 500. The decay traces of (b) **Rho-NDI**, (d) **Rho-Ph-NDI** and (f) **Rho-PhMe-NDI** at 475 nm excited in deaerated dimethylsilicone oil 500 with nanosecond pulsed laser**.** λ_{ex} = 355 nm. c = 5.0 × 10^{-5} M, 25 °C.

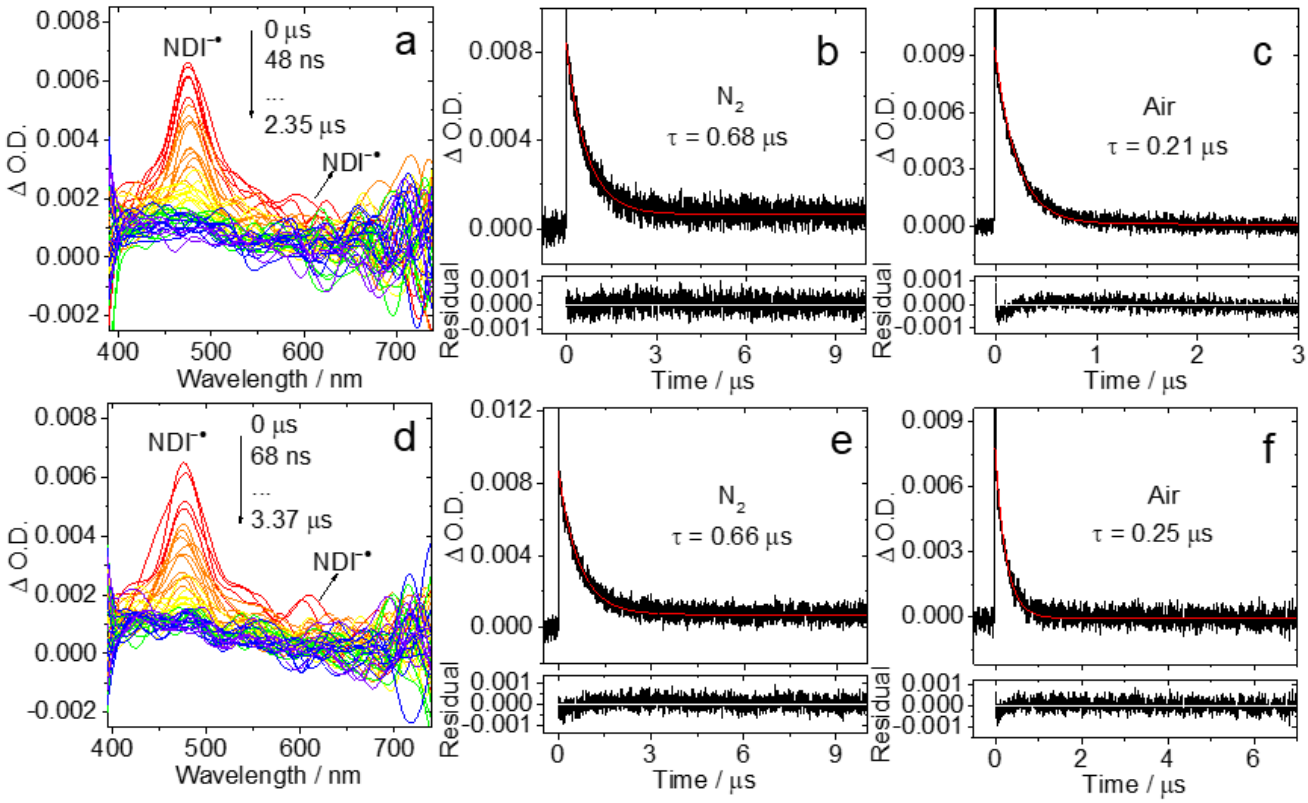

Fig. S38 Nanosecond transient absorption spectra of (a) **Rho-Ph-NDI** and (d) **Rho-PhMe-NDI** in deaerated viscous solvent triacetin. The decay traces of **Rho-Ph-NDI** (top row) and **Rho-PhMe-NDI** (bottom row) in (b, e) deaerated and (c, f) aerated triacetin at 470 nm excited with nanosecond pulsed laser**.** λ_{ex} = 355 nm. c = 3.0 × 10^{-5} M, 25 °C.

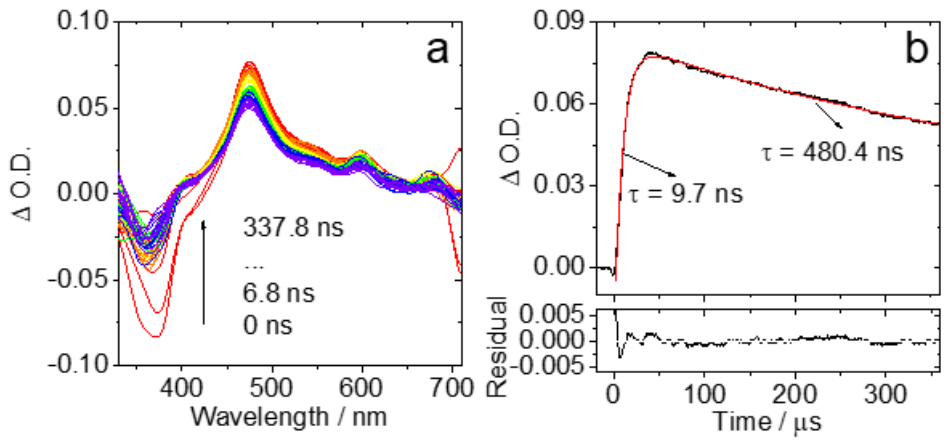

Fig. S39 (a) Nanosecond transient absorption spectra of **Rho-Ph-NDI** with kinetic mode and (b) the decay trace of **Rho-Ph-NDI** in deaerated ACN at 470 nm excited with nanosecond pulsed laser. λ_{ex} = 355 nm. c = 5.0 × 10^{-5} M, 25 °C.

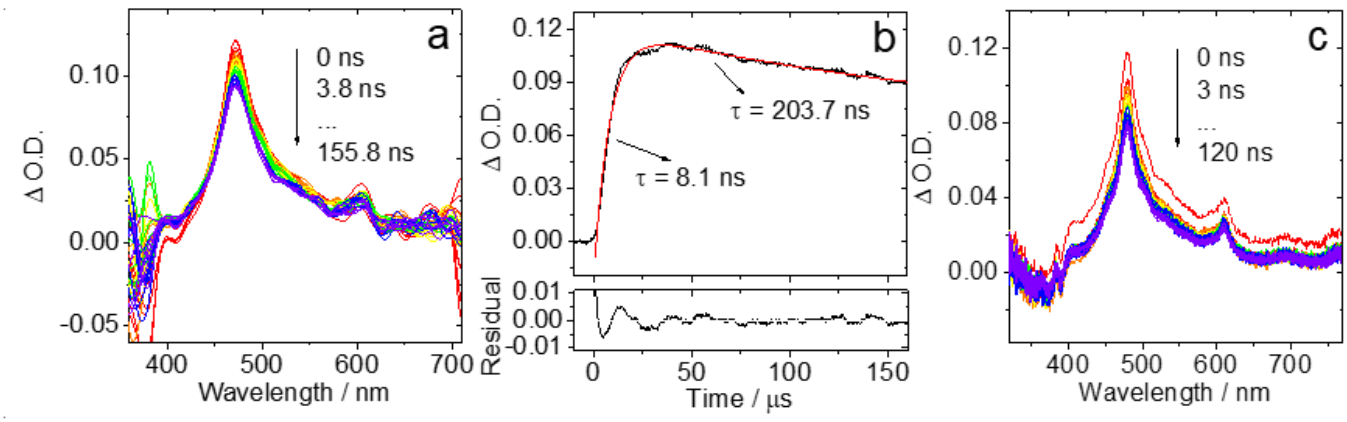

Fig. S40 Nanosecond transient absorption spectra of **Rho-PhMe-NDI** with (a) kinetic mode and (c) spectral mode; (b) and the decay trace of **Rho-PhMe-NDI** in deaerated ACN at 470 nm excited with nanosecond pulsed laser. λ_{ex} = 355 nm. c = 5.0 × 10^{-5} M, 25 °C.

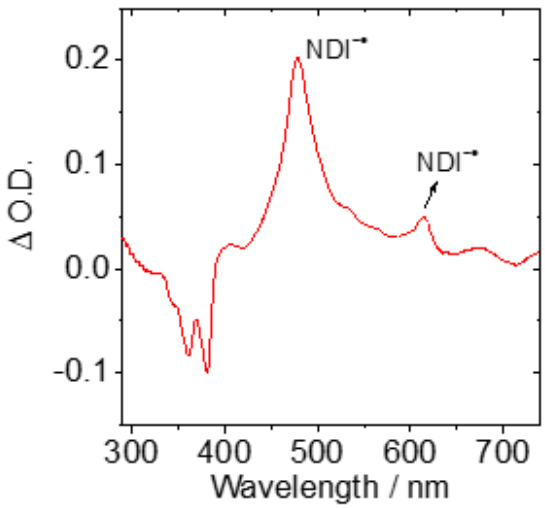

Fig. S41 Nanosecond transient absorption spectra of NDI in the presence of triethylamine (TEA). λ_{ex} = 355 nm. c[NDI] = 3.0 × 10^{-5} M, c[TEA] = 3.0 × 10^{-4} M, 25 °C.

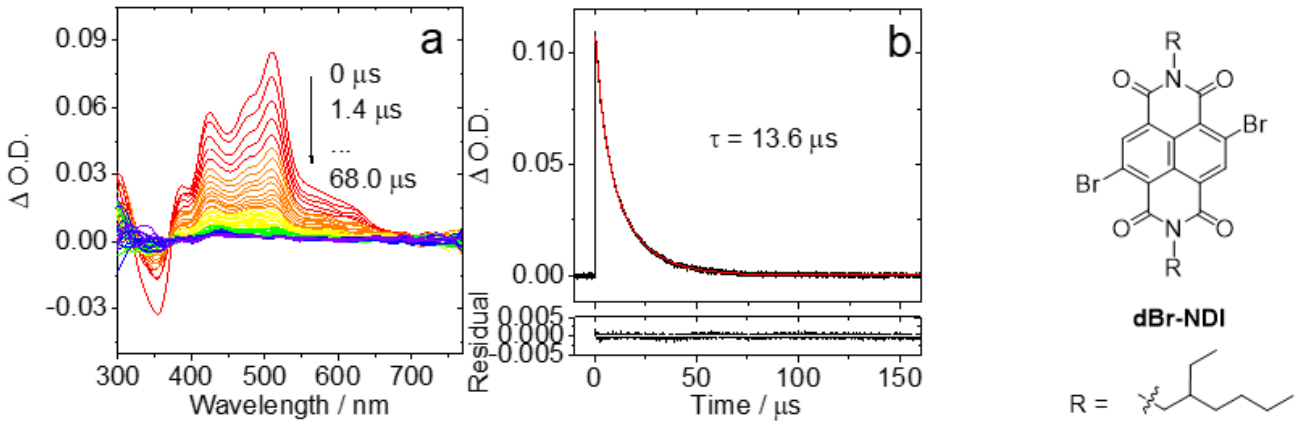

Fig. S42 (a) Nanosecond transient absorption spectra of dBr-NDI and (b) the decay trace at 510 nm in deaerated HEX excited with nanosecond pulsed laser. λ_{ex} = 355 nm. c = 4.0 × 10^{-5} M, 25 °C.

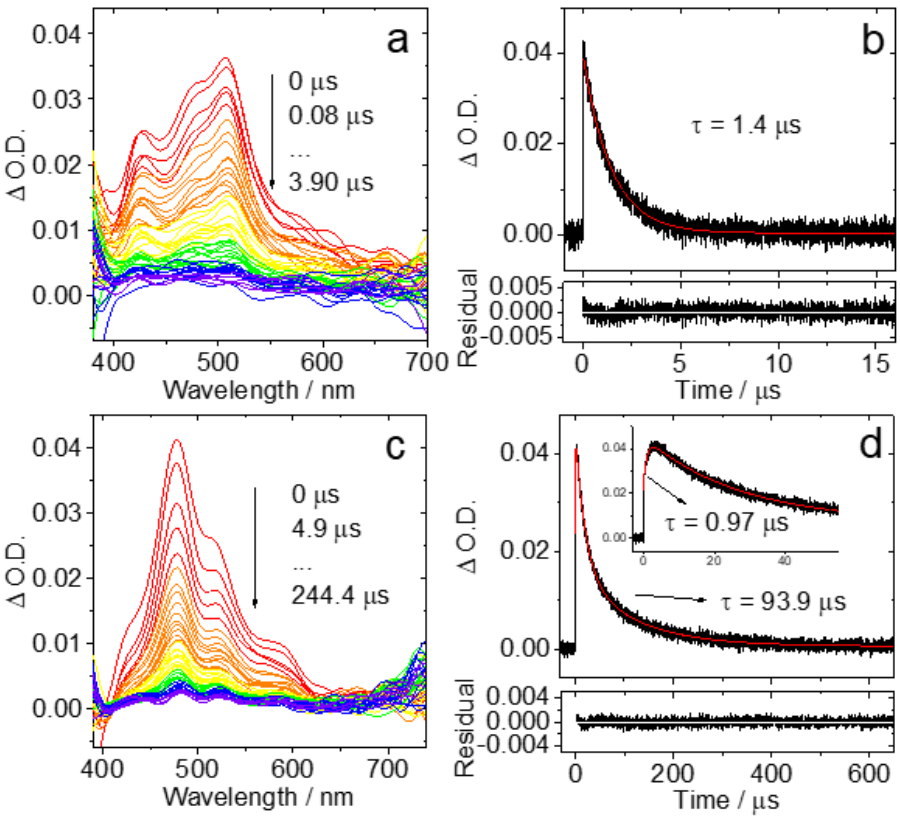

Fig. S43 Intermolecular triplet−triplet energy transfer (TTET) with dBr-NDI (c = 2 × 10^{-5} M) as the triplet photosensitizer and **Rho-NDI** (c = 8 × 10^{-5} M) as the triplet energy acceptor in different deaerated solvents (top row, in HEX; bottom row, in ACN). (a, c) Nanosecond transient absorption spectra of the mixture of dBr-NDI and **Rho-NDI** and the decay traces monitored at (b) 510 nm in HEX and (d) 470 nm in ACN. λ_{ex} = 355 nm, 25 °C.

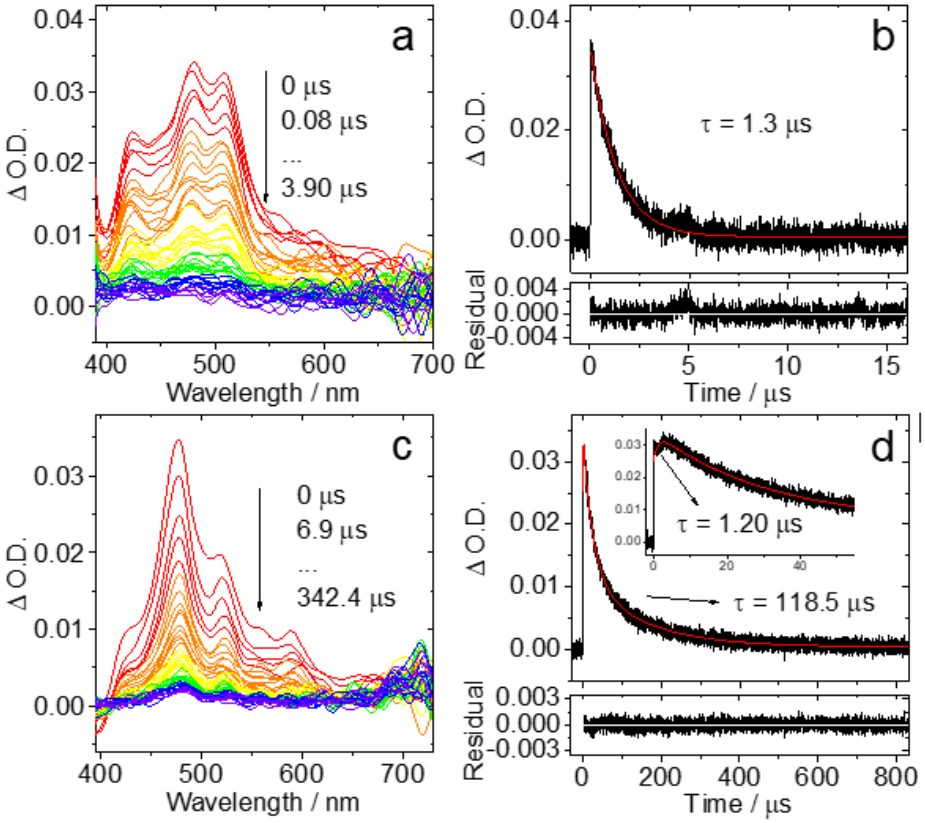

Fig. S44 Intermolecular TTET with dBr-NDI (c = 2 × 10^{-5} M) as the triplet photosensitizer and **Rho-Ph-NDI** (c = 8 × 10^{-5} M) as the triplet energy acceptor in different deaerated solvents (top row, in HEX; bottom row, in ACN). (a, c) Nanosecond transient absorption spectra of the mixture of dBr-NDI and **Rho-Ph-NDI** and the decay traces monitored at (b) 510 nm in HEX and (d) 470 nm in ACN. λ_{ex} = 355 nm, 25 °C.

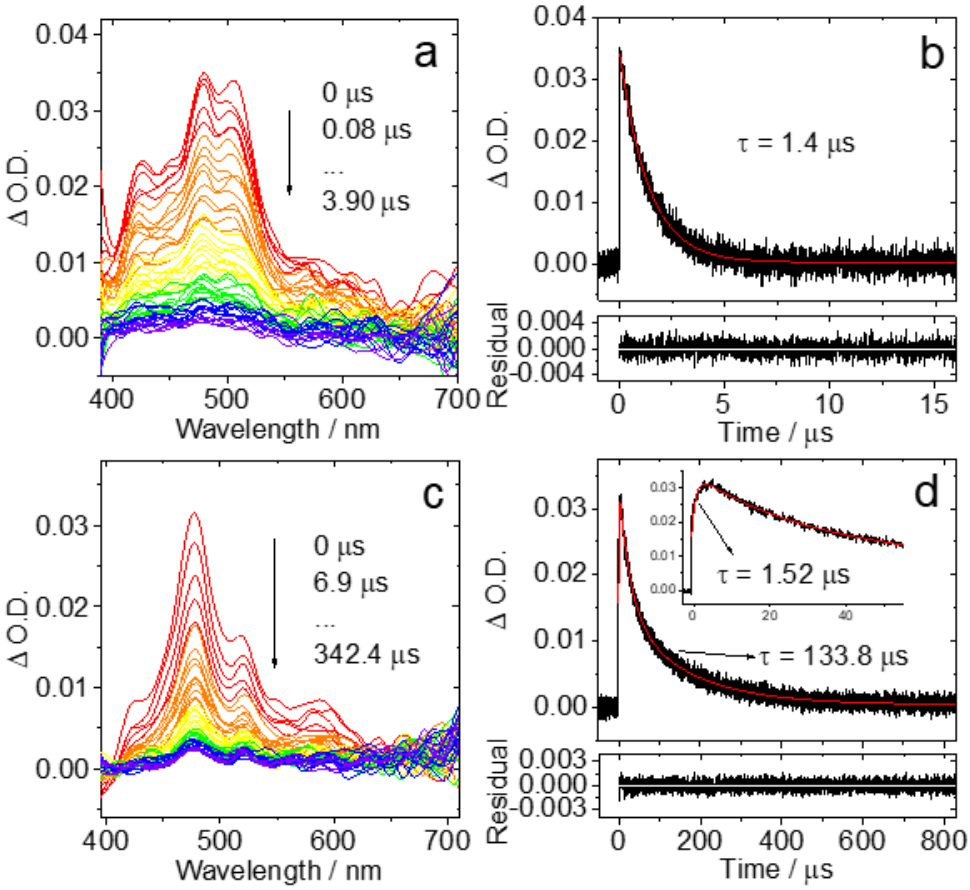

Fig. S45 Intermolecular TTET with dBr-NDI (c = 2 × 10^{-5} M) as the triplet photosensitizer and **Rho-PhMe-NDI** (c = 8 × 10^{-5} M) as the triplet energy acceptor in different deaerated solvents (top row, in HEX; bottom row, in ACN). (a, c) Nanosecond transient absorption spectra of the mixture of dBr-NDI and **Rho-PhMe-NDI** and the decay traces monitored at (b) 510 nm in HEX and (d) 470 nm in ACN. λ_{ex} = 355 nm, 25 °C.

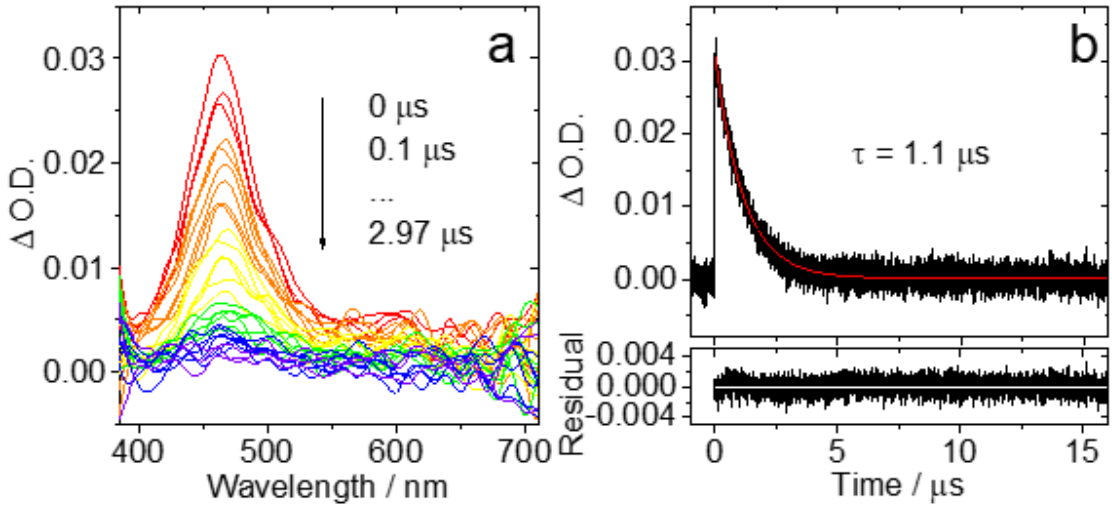

Fig. S46 Intermolecular electron transfer with PTZ (c = 8 × 10^{-5} M) as the electron donor and **Rho-NDI** (c = 8 × 10^{-5} M) as the electron acceptor in deaerated HEX. (a) Nanosecond transient absorption spectra of the mixture of PTZ and **Rho-NDI** and (b) the decay trace monitored at 470 nm. λ_{ex} = 355 nm, 25 °C.

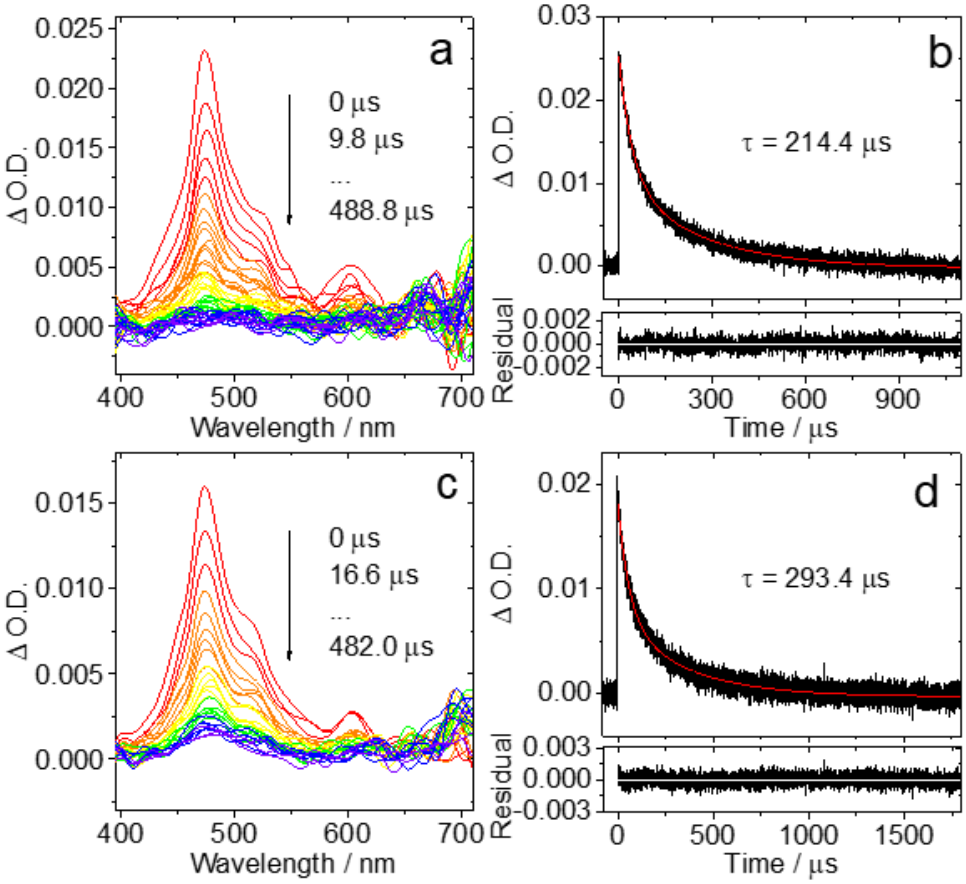

Fig. S47 Intermolecular TTET with PTZ (c = 2 × 10^{-5} M) as the electron donor and **Rho-Ph-NDI** or **Rho-PhMe-NDI** (c = 8 × 10^{-5} M) as the triplet energy acceptor in deaerated ACN (top row, **Rho-Ph-NDI**; bottom row, **Rho-PhMe-NDI**). (a, c) Nanosecond transient absorption spectra of the mixture and (b, d) the decay traces monitored at 470 nm. λ_{ex} = 355 nm, 25 °C.

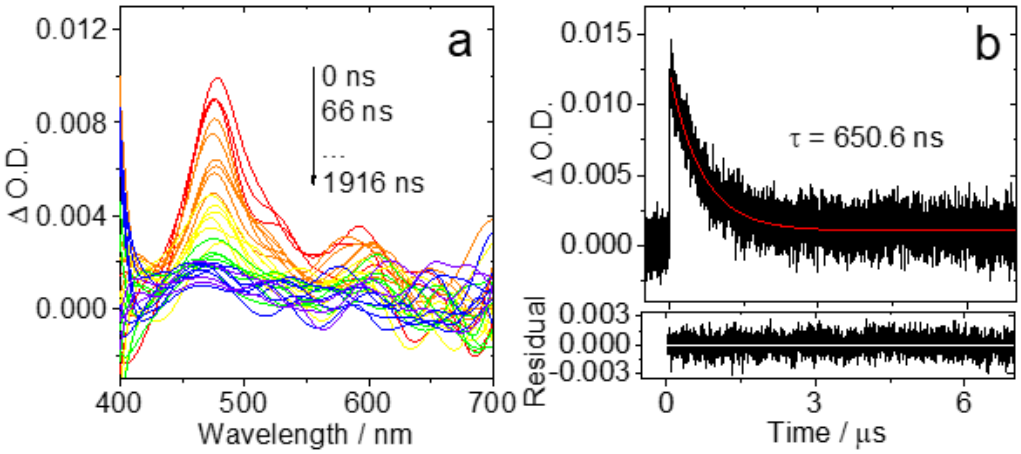

Fig. S48 Intermolecular TTET with TCNQ (c = 2 × 10^{-5} M) as the electron acceptor and **Rho-PhMe-NDI** (c = 8 × 10^{-5} M) as the triplet energy donor in deaerated ACN. (a) Nanosecond transient absorption spectra of the mixture and (b) the decay trace monitored at 470 nm. λ_{ex} = 355 nm, 25 °C.

10. Charge Transfer Quantum Yield

The charge transfer quantum yield was calculated with equation 1:

$$\Phi_{\mathrm{CS}} = \Phi_{\mathrm{std}} \left(\frac{\Delta \mathrm{O.D.}_{\mathrm{sam}}}{\Delta \mathrm{O.D.}_{\mathrm{std}}}\right)\left(\frac{\varepsilon_{\mathrm{std}}}{\varepsilon_{\mathrm{sam}}}\right) \qquad (1)$$

Where Φ_{std} is the triplet state quantum yield of the standard compound; ΔO.D.$_{\mathrm{sam}}$ and ΔO.D.$_{\mathrm{std}}$ are the ΔO.D. value of the sample' s radical anion/cation and the standard compound' s excited state at the maximal absorption in transient absorption spectra, respectively (with the fact that the sample' s radical anion/cation and the standard compound' s excited state does not overlap with the ground state bleaching band as the criterion); $\varepsilon_{\mathrm{sam}}$ and $\varepsilon_{\mathrm{std}}$ are the molar absorption coefficient of the sample' s radical anion/cation and the standard compound' s excited state. It should be noted that the absorption of the sample and the standard compound at the excited wavelength should be kept same. Anthracene was selected as standard compound, the Φ_{std} and $\varepsilon_{\mathrm{std}}$ of the triplet state of anthracene is 71% and 4.55×10^4 M^{-1} cm^{-1}, respectively; $\varepsilon_{\mathrm{std}}$, i.e. the molar absorption coefficient of the NDI radical anion, is 3.87×10^4 M^{-1} cm^{-1}, which was determined by chemical reduction with excess $CoCp_2$ as reductant. The excitation wavelength is 355 nm and the absorbance of the sample and the anthracene is 1.05 at 355 nm.

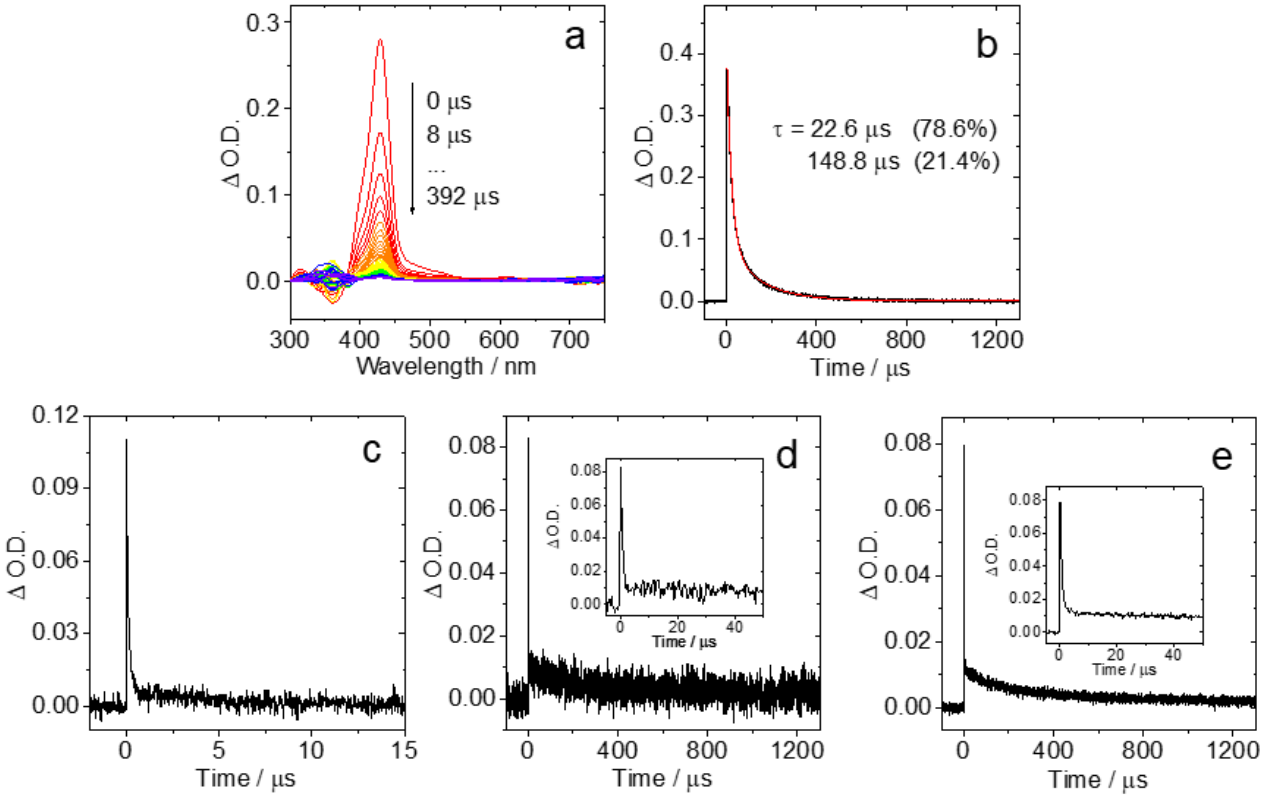

Fig. S49 (a) Nanosecond transient absorption spectra of anthracene and (b) the decay trace at 430 nm in deaerated TOL. The decay traces of (c) **Rho-NDI** in deaerated HEX and (d) **Rho-Ph-NDI** and (e) **Rho-PhMe-NDI** in ACN at 475 nm excited with nanosecond pulsed laser. λ_{ex} = 355 nm. A = 1.05 at 355 nm, 25 °C.

11. Time-Resolved Electron Paramagnetic Resonance Spectroscopy

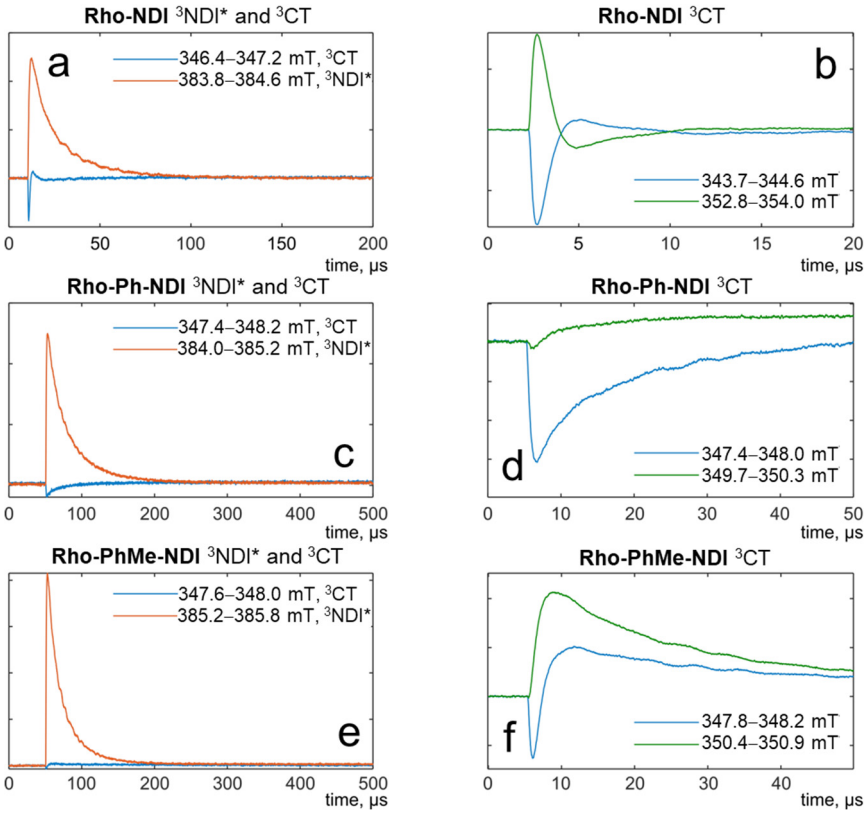

Fig. S50 The kinetics of the TREPR signal of the compounds. ^{3}NDI and ^{3}CT signal kinetics of (a) **Rho-NDI**, (c) **Rho-Ph-NDI** and (e) **Rho-PhMe-NDI** at absolute maxima of their spectra. Anisotropic evolutions of ^{3}CT spectra of (b) **Rho-NDI**, (d) **Rho-Ph-NDI** and (f) **Rho-PhMe-NDI**. The signal were recorded under 355 nm laser irradiation at 80 K in glassy TOL.

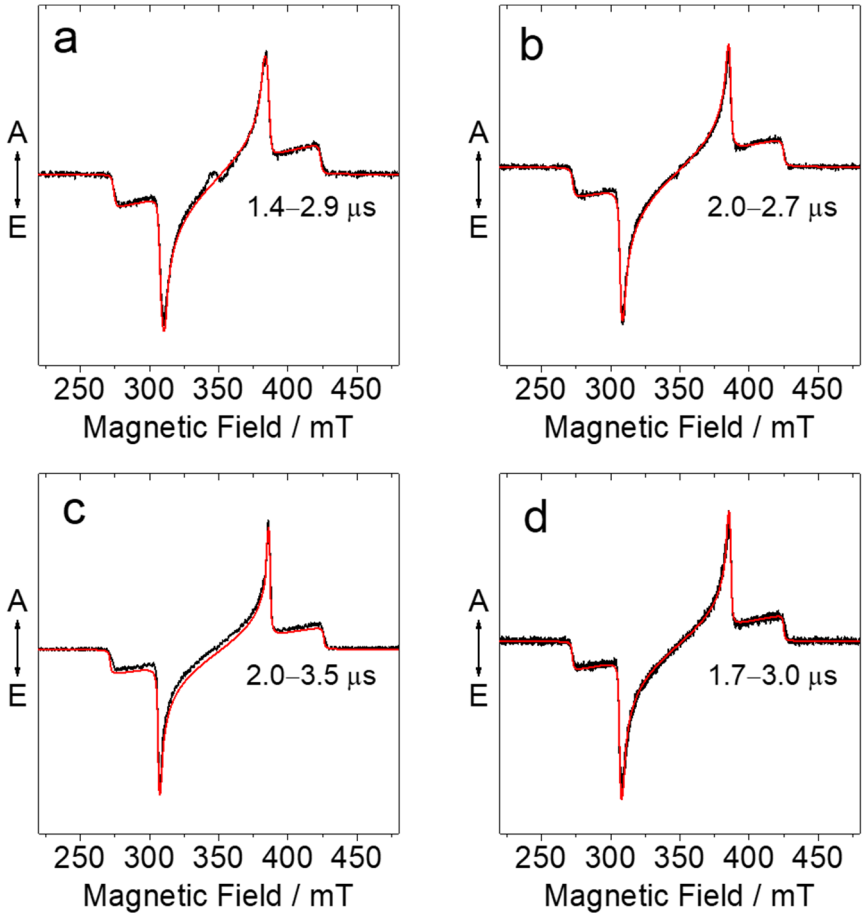

Fig. S51 TREPR spectra of (a) **Rho-NDI**, (b) **Rho-Ph-NDI**, (c) **Rho-PhMe-NDI** and (d) **NDI** at the maximum of main signal kinetics together with their simulations. Experiment is shown in black, simulations is shown in red. The spectra were obtained under 355 nm laser irradiation at 80 K in glassy toluene.

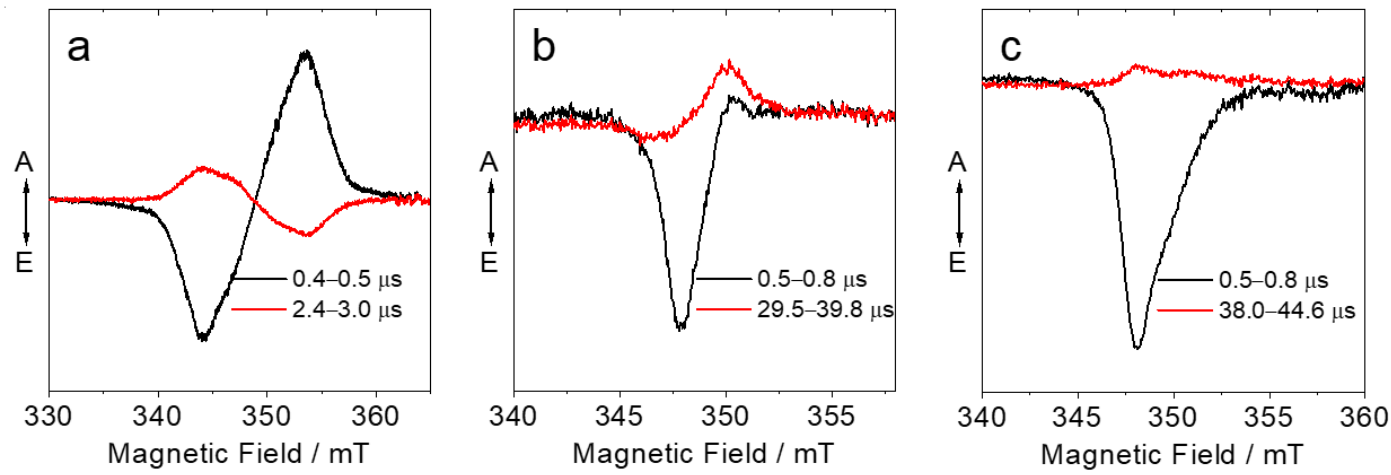

Fig. S52 TREPR spectra of (a) **Rho-NDI**, (b) **Rho-Ph-NDI** and (c) **Rho-PhMe-NDI** at different delay time after the laser flash. Experiment is shown in black, simulations of main signal is shown in red. The spectra were obtained under 355 nm laser irradiation at 80 K in glassy toluene.

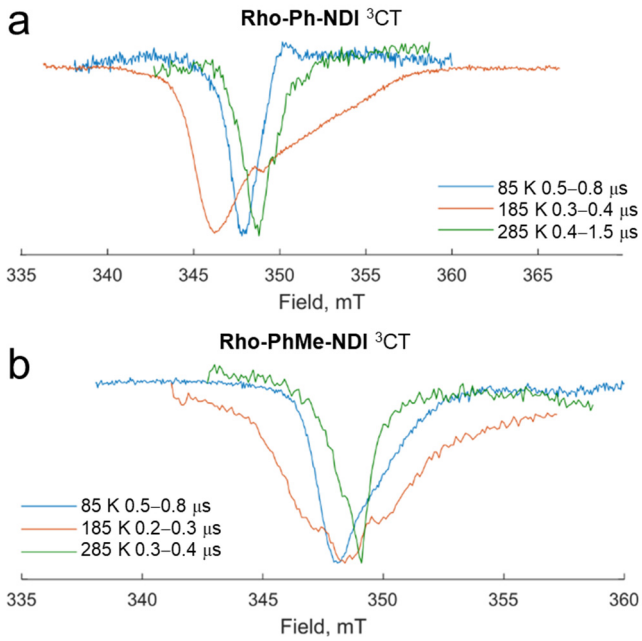

Fig. S53 TREPR spectra of narrow central-field range signals (presumably ^{3}CT) of (a) **Rho-Ph-NDI** and (b) **Rho-PhMe-NDI** in TOL at different temperatures. Spectra at 85 K are baseline corrected. The spectra were obtained under 355 nm laser irradiation.

12. DFT Calculation

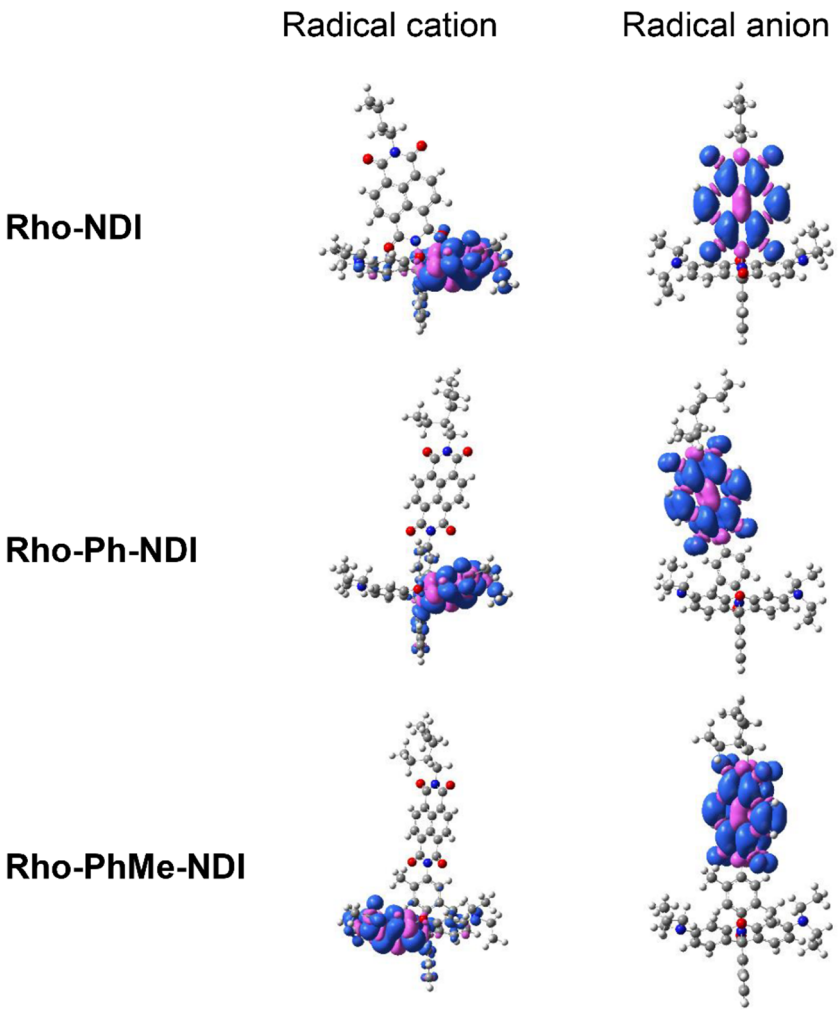

Fig. S54 Isosurfaces of spin density at the optimized radical cation and radical anion geometries of **Rho-NDI**, **Rho-Ph-NDI** and **Rho-PhMe-NDI**. Calculation was performed at CAM-B3LYP/6-31G(d) level with Gaussian 09W (Isovalue = 0.0004).

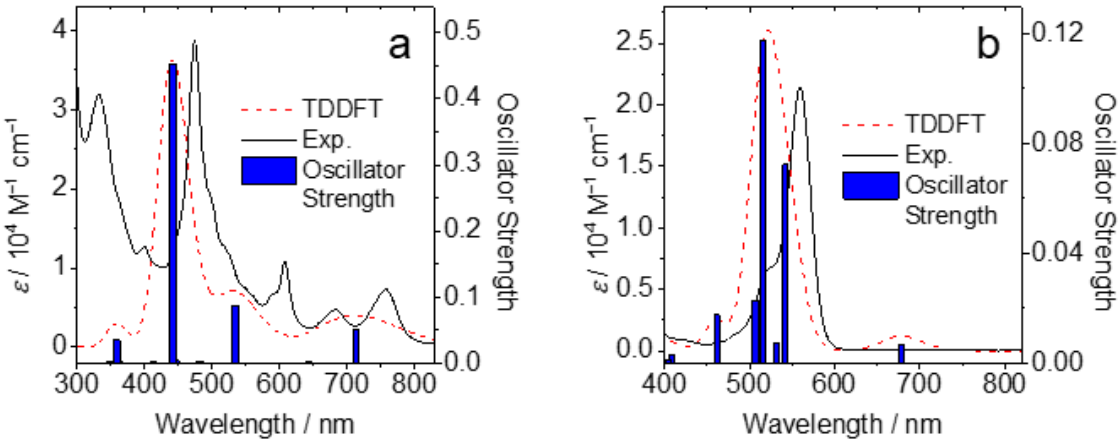

Fig. S55 Comparison of calculation and experimental data of UV–vis spectra for (a) $NDI^{-\bullet}$ and (b) $Rho^{+\bullet}$ of **Rho-NDI**. The calculations are performed by TDDFT at the (a) B3LYP/6-31G(d) level and (b) CAM-B3LYP/6-31G(d) level with Gaussian 09. The experimental data were measured by chemical redox.

Table S2 Lowest electronic excitation energies (eV) of ^{1}CT and ^{3}CT states of the dyads. The calculations are performed by DFT at the tuned CAM-B3LYP/6-31G(d) with Gaussian 16

Compounds	E_{1CT}/eV			E_{3CT}/eV		
	HEX	TOL	ACN	HEX	TOL	ACN
Rho-NDI	1.94	1.74	1.51	1.93	1.74	1.50
Rho-Ph-NDI	2.41	2.13	1.73	2.40	2.13	1.73
Rho-PhMe-NDI	2.28	2.03	1.74	2.27	2.02	1.74

Table S3 Hyperfine coupling constant of $NDI^{-\bullet}$ of the compounds by simulating the EPR spectra and DFT calculation (UB3LYP/EPR-II)[a]

HFC constant / G		α_{N1}	α_{N2}	α_{H1}	α_{H2}	α_{H3}	α_{H4}
NDI	Sim.	0.98	0.98	1.88	1.88	1.88	1.88
	DFT	1.03	1.04	1.82	1.82	1.87	1.87
Rho-NDI	Sim.	1.03	0.97	1.98	1.98	1.82	1.82
	DFT	1.07	1.01	1.95	1.95	1.76	1.76
Rho-Ph-NDI	Sim.	0.98	0.98	1.88	1.88	1.88	1.88
	DFT	1.02	1.00	1.83	1.83	1.88	1.88
Rho-PhMe-NDI	Sim.	0.98	0.98	1.88	1.88	1.88	1.88
	DFT	1.03	1.03	1.90	1.91	1.78	1.78

[a] The corresponding atoms were shown in Fig. S54.

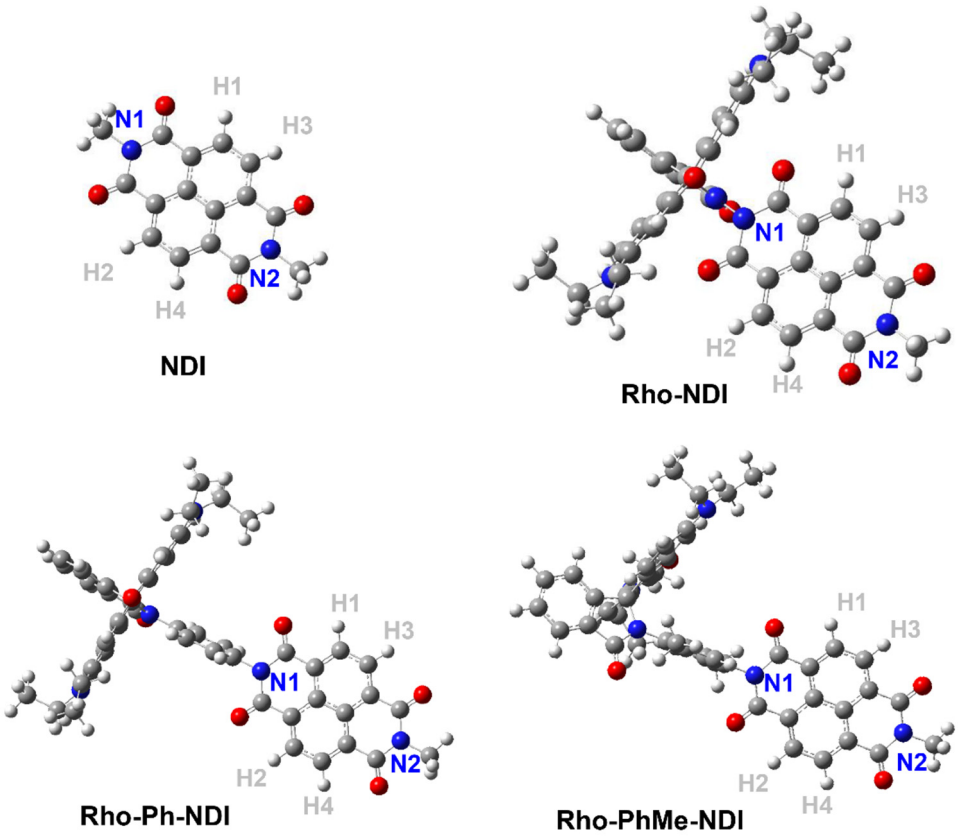

Fig. S56 The molecular structures for the DFT calculation of $NDI^{-\bullet}$ and the corresponding atoms acting on the EPR spectra of $NDI^{-\bullet}$.Calculation was performed at UB3LYP/EPR-II level with Gaussian 09.

13. Photophysical Process

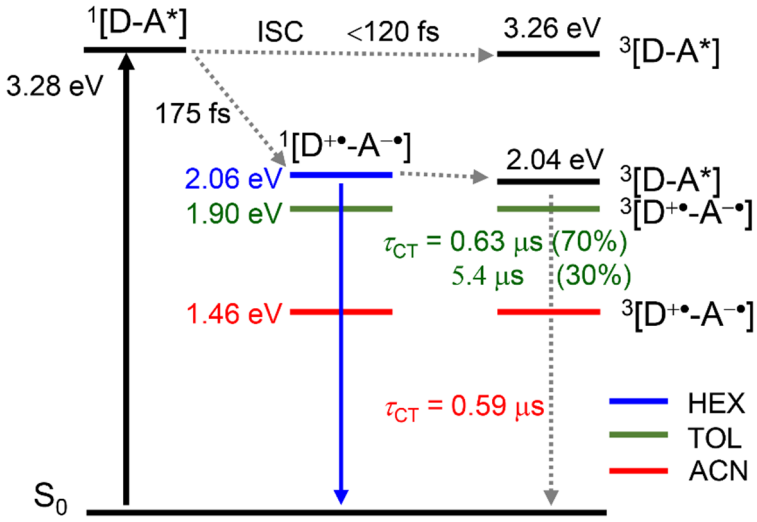

Scheme S1 Jablonski diagram showing the photophysical processes of **Rho-PhMe-NDI**. The energy of the excited singlet states is derived from the spectroscopic data; the energy of CT states is obtained by electrochemical calculation; and the triplet energy is estimated by TDDFT calculation. The number of the superscript designates the spin multiplicity.

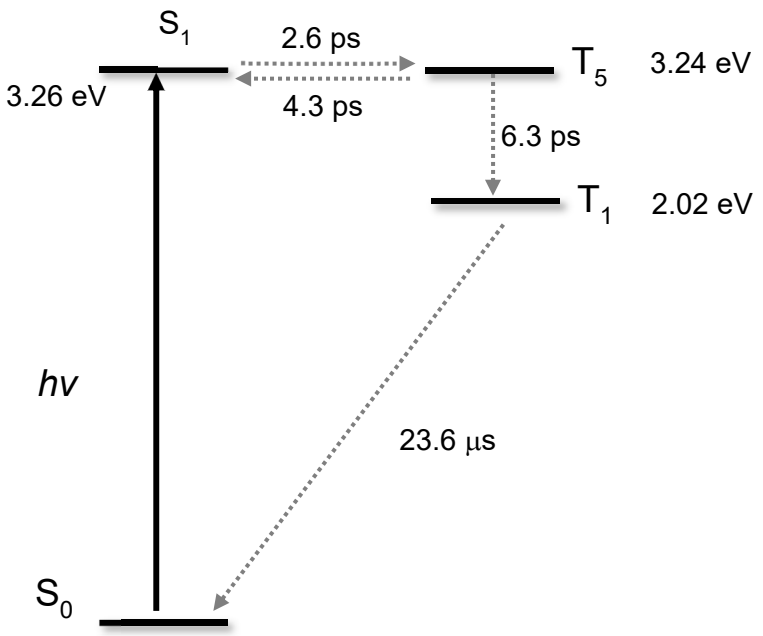

Scheme S2 Jablonski diagram showing the photophysical processes of **NDI**. The energy of the excited singlet states is derived from the spectroscopic data; and the triplet energy is estimated by TDDFT calculation. The number of the superscript designates the spin multiplicity.

14. Coordinates of the Optimized Geometries of the Molecules

Rho-NDI

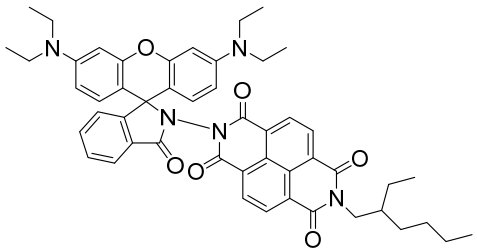

Calculation Type = FREQ
Calculation Method = RB3LYP
Basis Set = 6-31G(d)
Charge = 0
Spin = Singlet

E(RB3LYP) = −2503.988691 Hartree

RMS Gradient Norm = 0.000003 Hartree/Bohr
Imaginary Freq = 0
Dipole Moment = 6.070917 Debye
Polarizability (α) = 563.607763 a.u.
Point Group = C1

	X	Y	Z
C	3.523039	-2.48569	-1.38998
C	3.603669	-0.06471	-1.23238
C	2.200652	-0.006	-1.45476
C	1.477733	-1.20884	-1.64454
C	2.135402	-2.42821	-1.61813
C	1.557069	1.254818	-1.4964
C	3.679926	2.357652	-1.09936
H	4.043959	-3.43673	-1.36055
H	1.557917	-3.33323	-1.77293
H	4.260829	3.262925	-0.95889
C	0.090029	1.342903	-1.72767
C	0.009986	-1.17409	-1.88001
O	-0.49148	2.396793	-1.8797
O	-0.63751	-2.1614	-2.15809
C	2.292426	2.417147	-1.32793
H	1.775519	3.369678	-1.37295
N	-0.60574	0.101155	-1.72756
C	-2.54746	-3.58086	1.510904
C	-3.0574	-3.59224	0.185264
C	-3.20035	-2.41981	-0.5333
C	-2.87395	-1.16118	-0.00324
C	-2.40167	-1.154	1.309435
C	-2.24443	-2.3222	2.059596
C	-2.98222	0.115924	-0.81938
C	-2.85593	1.324137	0.093685

C	-2.3938	1.207986	1.404451
O	-2.07787	0.000634	1.978905
C	-3.1422	2.626326	-0.34599
C	-2.98175	3.737273	0.460253
C	-2.50814	3.61293	1.793746
C	-2.20871	2.313609	2.238756
N	-2.37607	4.727262	2.627353
N	-2.33683	-4.76344	2.2248
C	-1.84525	-4.64867	3.601492
C	-3.10528	-5.95745	1.865244
C	-4.24991	0.16224	-1.67616
C	-3.94993	0.21637	-3.03687
C	-2.47838	0.208064	-3.2283
C	-5.57485	0.159739	-1.25056
C	-6.58215	0.210951	-2.21833
C	-6.2742	0.264505	-3.58577
C	-4.94552	0.268041	-4.00956
O	-1.82494	0.239619	-4.2542
C	-4.58571	-5.90995	2.268448
C	-1.36552	-5.95883	4.227122
C	-1.82612	4.509429	3.969308
C	-2.18738	6.045323	2.01458
C	-0.8181	6.252058	1.351981
C	-1.95411	5.699546	4.920804
H	-3.32136	-4.52305	-0.29961
H	-3.55879	-2.47845	-1.55582
H	-1.90492	-2.19935	3.078722
H	-3.48558	2.769702	-1.36543
H	-3.22237	4.707588	0.04588
H	-1.82172	2.112227	3.22801
H	-0.99218	-3.96274	3.58057
H	-2.60041	-4.1858	4.261022
H	-3.01366	-6.12424	0.788838
H	-2.62165	-6.81946	2.328627
H	-5.8202	0.119262	-0.1932
H	-7.62287	0.209392	-1.90511
H	-7.07754	0.303677	-4.31618
H	-4.6772	0.309213	-5.06102
H	-5.09662	-6.82993	1.960449
H	-4.69791	-5.8098	3.354284
H	-5.0934	-5.0624	1.796669
H	-0.88004	-5.73225	5.182523
H	-2.18157	-6.65765	4.43634
H	-0.63177	-6.46088	3.587188
H	-2.38085	3.675571	4.411399

H	-0.76962	4.191151	3.923573
H	-2.98626	6.213304	1.287255
H	-2.34429	6.79902	2.788316
H	-0.75225	7.255375	0.914626
H	-0.00602	6.148568	2.081169
H	-0.65395	5.519934	0.554652
H	-1.66275	5.376134	5.925972
H	-1.3042	6.537326	4.649176
H	-2.98705	6.060983	4.969173
N	-1.96361	0.155316	-1.9376
C	4.331689	1.135741	-1.05029
C	4.251951	-1.32283	-1.19865
C	5.79728	1.087891	-0.80299
C	5.717024	-1.39887	-0.95533
O	6.459966	2.097989	-0.61308
O	6.313615	-2.46461	-0.89414
N	6.3975	-0.18109	-0.79775
C	7.852202	-0.2436	-0.55124
H	8.282054	0.664765	-0.97571
H	8.226563	-1.11222	-1.09492
C	8.191616	-0.35482	0.938885
H	7.765911	0.50797	1.466943
H	7.715499	-1.25598	1.34592
C	9.70501	-0.41407	1.18275
H	10.17684	0.484145	0.760175
H	10.12829	-1.26947	0.637765
C	10.0626	-0.52729	2.668097
H	11.14788	-0.5651	2.814474
H	9.679055	0.330555	3.233735
H	9.634244	-1.43486	3.110498

Rho-Ph-NDI

Calculation Type = FREQ
Calculation Method = RB3LYP
Basis Set = 6-31G(d)
Charge = 0
Spin = Singlet

E(RB3LYP) = −2892.321564 Hartree

RMS Gradient Norm = 0.000001 Hartree/Bohr
Imaginary Freq = 0
Dipole Moment = 6.575386 Debye
Polarizability (α) = 690.882817 a.u.

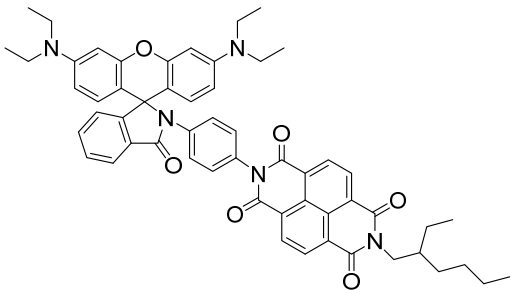

Point Group = C1

	X	Y	Z
C	-5.53063	2.086755	-1.69906
C	-5.43686	-0.27181	-1.13574
C	-4.02135	-0.24234	-1.26133
C	-3.37927	0.970551	-1.60875
C	-4.12873	2.116267	-1.82383
C	-3.27856	-1.42689	-1.03959
C	-5.33353	-2.63183	-0.5828
H	-6.12385	2.979402	-1.86656
H	-3.61167	3.032045	-2.08982
H	-5.85071	-3.54935	-0.32339
C	-1.79451	-1.41614	-1.16592
C	-1.89731	1.021046	-1.747
O	-1.11867	-2.4126	-0.97734
O	-1.30597	2.044621	-2.04159
C	-3.93141	-2.60263	-0.70512
H	-3.33885	-3.49642	-0.5416
N	-1.20216	-0.1856	-1.51825
C	5.372413	3.640197	1.435106
C	5.396091	3.639461	0.015254
C	5.383154	2.453246	-0.69781
C	5.346445	1.198474	-0.0742
C	5.333651	1.202245	1.320724
C	5.3564	2.382559	2.066538
C	5.39245	-0.10195	-0.86998
C	5.148449	-1.29229	0.04499
C	5.148379	-1.1614	1.432925
O	5.29975	0.049118	2.071147
C	4.965965	-2.58858	-0.45748
C	4.79131	-3.68757	0.364801
C	4.803927	-3.55202	1.777525
C	4.974231	-2.25237	2.287218
N	4.680635	-4.66456	2.617329
N	5.333462	4.82972	2.166107
C	5.348602	4.730951	3.629323
C	5.84985	6.056304	1.553714
C	6.746261	-0.2212	-1.57037
C	6.582221	-0.21389	-2.9467
C	5.143523	-0.13068	-3.27435
C	8.017325	-0.31015	-1.00992
C	9.111156	-0.39335	-1.87502
C	8.940233	-0.38352	-3.26875

C	7.664331	-0.29285	-3.82213
O	4.661652	-0.10664	-4.39796
C	7.378557	6.112522	1.427893
C	5.027047	6.030716	4.367614
C	4.731633	-4.43012	4.06376
C	3.894073	-5.81204	2.150047
C	2.378636	-5.57262	2.112706
C	4.922281	-5.69083	4.908525
H	5.412633	4.568257	-0.5401
H	5.391525	2.498014	-1.7833
H	5.365423	2.273189	3.142144
H	4.956447	-2.73497	-1.53398
H	4.660433	-4.65762	-0.09727
H	4.948627	-2.03855	3.346883
H	4.585412	3.997614	3.909399
H	6.311936	4.333417	3.994568
H	5.386127	6.182028	0.571755
H	5.49423	6.901615	2.145575
H	8.158521	-0.31656	0.067191
H	10.11349	-0.46732	-1.46143
H	9.810324	-0.44883	-3.9161
H	7.499089	-0.2851	-4.89533
H	7.689548	7.051106	0.954083
H	7.859736	6.056221	2.411275
H	7.753419	5.282505	0.820264
H	4.912244	5.806868	5.433661
H	5.818251	6.781735	4.277951
H	4.087977	6.468604	4.012393
H	5.589433	-3.77625	4.249724
H	3.83954	-3.88421	4.418901
H	4.251087	-6.1054	1.159959
H	4.123696	-6.65987	2.798736
H	1.859137	-6.4689	1.753825
H	1.988393	-5.33497	3.109201
H	2.127668	-4.74302	1.443951
H	5.123103	-5.39318	5.943427
H	4.037703	-6.33536	4.923734
H	5.775689	-6.27903	4.554034
N	4.454731	-0.09354	-2.05154
C	-6.08173	-1.48406	-0.79322
C	-6.18088	0.910921	-1.35909
C	-7.56303	-1.53141	-0.66264
C	-7.66186	0.891321	-1.23228
O	-8.1518	-2.5692	-0.39312
O	-8.3452	1.884728	-1.43691

N	-8.25728	-0.32673	-0.86359
C	-9.73335	-0.33916	-0.76083
H	-10.0401	-1.38014	-0.85993
H	-10.1083	0.225193	-1.61748
C	-11.81	0.456966	0.378151
H	-12.2669	-0.52661	0.200904
H	-11.9956	1.04317	-0.53342
C	-12.5403	1.137528	1.548807
H	-13.6171	1.130636	1.327255
H	-12.4216	0.543387	2.465465
C	2.215754	-0.41869	-3.02325
C	3.040539	-0.10142	-1.92529
C	2.425656	0.18476	-0.69319
C	1.040789	0.154853	-0.56293
C	0.23942	-0.15726	-1.65551
C	0.8323	-0.44168	-2.88201
H	3.016848	0.441155	0.172377
H	0.211126	-0.68755	-3.73817
C	-10.282	0.289006	0.538386
H	-9.84291	1.291738	0.605004
C	-12.1057	2.584307	1.823088
H	-11.0433	2.610361	2.099216
H	-12.1921	3.168473	0.895843
C	-9.86837	-0.4786	1.814392
H	-8.77334	-0.56071	1.832749
H	-10.1268	0.140311	2.683565
C	-10.4756	-1.87602	1.996161
H	-10.1852	-2.55062	1.185127
H	-10.1219	-2.32158	2.933137
H	-11.5699	-1.8434	2.044056
C	-12.9293	3.253028	2.928863
H	-12.6003	4.28342	3.105787
H	-13.9942	3.283276	2.66713
H	-12.8383	2.707305	3.876334
H	0.586293	0.380111	0.397056
H	2.661278	-0.63062	-3.98286

Rho-PhMe-NDI

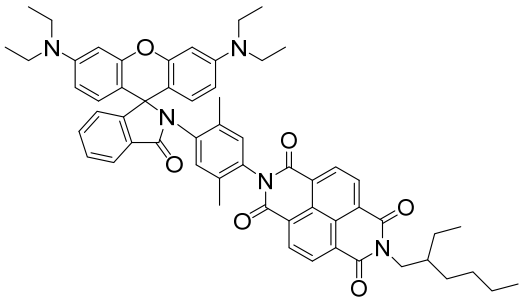

Calculation Type = FREQ
Calculation Method = RB3LYP
Basis Set = 6-31G(d)
Charge = 0
Spin = Singlet

E(RB3LYP) = –2970.955825 Hartree

RMS Gradient Norm = 0.000003 Hartree/Bohr
Imaginary Freq = 0
Dipole Moment = 6.549523 Debye
Polarizability (α) = 705.536944 a.u.
Point Group = C1

	X	Y	Z
C	-5.03659	2.062644	0.499155
C	-5.29675	0.290045	-1.13759
C	-3.88399	0.151071	-1.20668
C	-3.06324	0.983387	-0.40845
C	-3.63734	1.924227	0.431822
C	-3.32172	-0.81622	-2.07352
C	-5.54543	-1.47873	-2.77968
H	-5.49318	2.79797	1.153055
H	-2.9854	2.549407	1.032515
H	-6.19648	-2.10108	-3.38417
C	-1.8437	-0.97345	-2.16204
C	-1.58065	0.854749	-0.46963
O	-1.32166	-1.80705	-2.88233
O	-0.84106	1.542308	0.212741
C	-4.14613	-1.61818	-2.84678
H	-3.68975	-2.35082	-3.5038
N	-1.06723	-0.10777	-1.3646
C	4.834101	3.708998	1.198559
C	5.457373	3.584923	-0.0718
C	5.680855	2.340817	-0.63613
C	5.321518	1.142458	0.000166
C	4.74754	1.271562	1.265167
C	4.512543	2.511709	1.862216
C	5.510463	-0.21384	-0.65934
C	5.329454	-1.31547	0.374641
C	4.761981	-1.06533	1.624362
O	4.400026	0.191009	2.038756

C	5.643526	-2.65503	0.096969
C	5.401305	-3.68109	0.99372
C	4.823683	-3.42028	2.266
C	4.500722	-2.08056	2.548311
N	4.617005	-4.43936	3.198633
N	4.53998	4.957653	1.751349
C	3.914839	4.985344	3.077581
C	5.325109	6.122202	1.336472
C	6.857276	-0.3349	-1.36945
C	6.67932	-0.57356	-2.727
C	5.227318	-0.61081	-3.04041
C	8.138115	-0.25107	-0.83033
C	9.228161	-0.40979	-1.69086
C	9.042851	-0.65147	-3.06061
C	7.757034	-0.73677	-3.59452
O	4.708239	-0.79711	-4.13194
C	6.756842	6.157829	1.889364
C	3.345702	6.342191	3.493277
C	3.946339	-4.08436	4.454238
C	4.502536	-5.82113	2.724388
C	3.194721	-6.13755	1.985538
C	3.970843	-5.16938	5.531071
H	5.75742	4.461808	-0.63092
H	6.154771	2.290959	-1.61266
H	4.090647	2.496041	2.857456
H	6.081053	-2.90041	-0.86676
H	5.671864	-4.68804	0.703376
H	4.033009	-1.77889	3.475204
H	3.083663	4.273592	3.053505
H	4.610343	4.62783	3.857461
H	5.343134	6.164615	0.244334
H	4.784771	7.018591	1.646717
H	8.287921	-0.06714	0.229861
H	10.23706	-0.34601	-1.29159
H	9.908607	-0.7722	-3.70604
H	7.581974	-0.92301	-4.65006
H	7.283237	7.051276	1.533039
H	6.758362	6.180862	2.985279
H	7.323223	5.277134	1.569329
H	2.769159	6.210862	4.415284
H	4.120281	7.087804	3.699205
H	2.671043	6.741505	2.728302
H	4.46467	-3.20937	4.859753
H	2.902717	-3.77209	4.274557
H	5.360535	-6.04545	2.08489

H	4.610599	-6.48097	3.586947
H	3.184178	-7.18285	1.654975
H	2.325256	-5.98085	2.634459
H	3.077909	-5.50011	1.103138
H	3.580642	-4.74437	6.462105
H	3.347052	-6.03407	5.283346
H	4.991205	-5.51885	5.722714
N	4.569004	-0.38481	-1.84029
C	-6.11886	-0.53897	-1.93737
C	-5.85985	1.258191	-0.27303
C	-7.59907	-0.40018	-1.88099
C	-7.33618	1.415265	-0.19587
O	-8.33554	-1.08213	-2.57995
O	-7.86379	2.254499	0.520443
N	-8.11434	0.553306	-0.98646
C	-9.58157	0.732824	-0.9175
H	-9.98867	0.28935	-1.82585
H	-9.76318	1.809758	-0.93529
C	-11.7016	0.615897	0.400283
H	-12.2316	0.274477	-0.49975
H	-11.7012	1.714433	0.350677
C	-12.5066	0.186772	1.63925
H	-13.5364	0.55221	1.517622
H	-12.5833	-0.90866	1.678773
C	2.433189	0.716991	-2.40634
C	3.145007	-0.30417	-1.74324
C	2.457766	-1.25721	-0.9816
C	1.071023	-1.22753	-0.81692
C	0.376857	-0.20914	-1.47773
C	1.043833	0.729934	-2.25735
H	3.019928	-2.05628	-0.51441
H	0.465489	1.503256	-2.75491
C	0.368649	-2.2712	0.015169
H	-0.30163	-1.81431	0.752891
H	-0.2343	-2.93662	-0.61435
H	1.094388	-2.88356	0.558142
C	3.102417	1.759766	-3.26423
H	3.934516	2.23624	-2.73633
H	3.50442	1.307013	-4.17673
H	2.389547	2.540963	-3.5453
C	-10.235	0.131397	0.345475
H	-9.70993	0.570041	1.20227
C	-11.9573	0.704454	2.976064
H	-10.9474	0.307775	3.145031
H	-11.8489	1.797223	2.92337

C	-10.0791	-1.40242	0.448509
H	-9.01026	-1.64882	0.390164
H	-10.3918	-1.71032	1.454835
C	-10.839	-2.23806	-0.59023
H	-10.5128	-2.00771	-1.60879
H	-10.6553	-3.30562	-0.42242
H	-11.922	-2.08139	-0.5297
C	-12.8478	0.335159	4.167294
H	-12.4346	0.714416	5.108957
H	-13.856	0.752437	4.053485
H	-12.9506	-0.75295	4.263369

15. References

1. D. Liu, A. M. El - Zohry, M. Taddei, C. Matt, L. Bussotti, Z. Wang, J. Zhao, O. F. Mohammed, M. Di Donato and S. Weber, *Angew. Chem., Int. Ed.*, 2020, **59**, 11591–11599.
2. K. Chen, J. Zhao, X. Li and G. G. Gurzadyan, *J. Phys. Chem. A*, 2019, **123**, 2503–2516.
3. W. Wang, X. Wang, Q. Yang, X. Fei, M. Sun and Y. Song, *Chem. Commun.*, 2013, **49**, 4833–4835.
4. M. Kondratenko, A. G. Moiseev and D. F. Perepichka, *J. Mater. Chem.*, 2011, **21**, 1470–1478.
5. R. Narayana, P. Kumar, K. S. Narayand and S. K. Asha, *J. Mater. Chem. C*, 2014, **2**, 6511–6519.